TURBULENT NATURAL CONVECTION IN AN ENCLOSURE USING TWO EQUATION $k-\omega$ TURBULENCE MODEL AND PISO METHOD

BY

JANETH BOSIBORI OMWENGA (Bsc)

REG NO.156/CE/39530/2016

A project submitted for partial fulfillment for the degree of Master of Science in Applied Mathematics in the school of pure and applied sciences, Department of Mathematics of Kenyatta University.

2021

DECLARATION

I Janeth Bosibori Omwenga declare that this project is my original work and has not been done in any other institution for consideration of any certification.

JANETH BOSIBORI OMWENGA

REG. NO.156/CE/39530/2016

KENYATTA UNIVERSITY

SIGNATURE _____ DATE_____

I confirm that the student under my guidance and supervision carried out the work in the project.

DR. AWUOR KENNEDY OTIENO

SCHOOL OF PURE AND APPLIED SCIENCES

KENYATTA UNIVERSITY

SIGNATURE_____ DATE_____

DEDICATION

I dedicate this project to my mama Joyce Nyanchera, my papa Mark Omwenga, my late husband Paul Mose, my daughters Ekkaterrinah Syombbua and Leticia Bosibori and my sons Emmanuel Nikola and Paul Mose, who, through their love, prayer, inspiration, support, and encouragement, have been instrumental in inspiring me to complete this study as well as assisting me in overcoming all of the study's difficulties.

ACKNOWLEDGEMENTS

I highly appreciate my supervisor Dr. Awuor Kennedy Otieno of Kenyatta University who has been generous with his time and energy on matters of academic during my entire study.

I extend acknowledgement to all the lecturers in mathematics Department for guidance, encouragement and support throughout this program. Special thanks to my late husband for his financial support and encouragement to run this race, I wonder where I will be without him! Above all I give thanks to almighty God for who I am today and for giving me the gift of life, good health and patience.

ABSTRACT

The natural convection on a surface depends on the geometry as well as its orientation. In natural convection, the motion of the fluid takes place by natural means such as gravitational force and buoyancy. Turbulent natural convection in an enclosure has been studied in the past but so far the prediction of heat transfer within an enclosure has not been completely established. The aim of this study is to predict the transfer of heat as a result of natural convection inside a square cavity filled with air using k-omega. Natural turbulent convection in square air cavities having isothermal vertical wall and highly-heat conductivity horizontal wall was carried out. The distribution of the temperature and velocity in the enclosure was determined for various Rayleigh numbers .The process involved numerically simulating the flow of the fluid inside an enclosure using the k-omega turbulence model and since pressure gradient was considered in the momentum equation the PISO Method was used. It was found out that in an enclosure environment, the natural turbulence flow is responsible for temperature distribution. Temperature profiles are important for thermal comfort (including air velocity, temperature and humidity levels), efficiency of energy balance and the effectiveness of the ventilation system when modeling air flow in buildings.

TABLE OF CONTENTS

LIST OF TABLES

LIST OF FIGURES

NOMENCLATURE

A_1, A_2, A_3	**Dimensionless Parameter**
A	**Aspect ratio**
B_1, B_2, B_3, B_4	**Dimensionless Parameter**
C_p	**Specific heat at constant pressure**
C_μ	**Empirical constant**
e	**Specific internal energy**
F	**Body force**
g	**Acceleration due to gravity**
G_k	**Buoyant production of turbulent kinetic energy**
h	**Mesh interval/Static enthalpy**
i, j, k	**Integer variables**
k	**Kinetic energy of turbulence**
L_1, L_2, L_3	**Dimensionless parameters**
n	**Co-ordinate normal to the boundary**
N_u	**Nusselt number**

P	**Thermodynamic pressure**
P_k	**Shear production of turbulent kinetic energy**
Q	**Non-dimensional heat transfer**
q_j	**Conductor vector**
s	**Specific entropy**
S_Q	**Source terms**
t	**Time**
T	**Thermodynamic temperature**
T_0	**Reference temperature**
u, u', U	**Instantaneous /fluctuation/mean velocity in x-direction**
U_*	**Characteristic velocity**
v, v', V	**Instantaneous/fluctuation/mean velocity in y-direction**
w, w', W	**Instantaneous/fluctuation/mean velocity in z-direction**
$(p_o^2 C_{Po} g\beta \Delta T L_0)/(\mu_0 K_0) = Ra$	**Rayleigh-number**
$(\mu_0 C_{Po})/(\mu_0 C_{Po}) = Pr$	**Prandtl number**

$(\mu_0 g/\rho_0)/(\mu_0 g/\rho_0) = Gn$	**Gravity number**
$P_0/(P_0 U_*^2) = Eu$	**Euler number**
$P_0/(C_{Po}\rho_0 T_0) = Pn$	**Pressure number**
$P_0 U_* L_0/\mu_0 = Re$	**Reynolds number**
$U_*/gL_0 = F_r$	**Froude number**
$\zeta = \Delta T_*/T_0$	**Non-dimensional temperature Difference**
$\eta = \beta_0 T_0, R_a/P_r = Gr$	**Grashof number**

GREEK SYMBOLS

α	**The thermal expansion coefficient**
β	**Coefficient of volumetric expansion**
∇	**Gradient operator**
Δt	**Time interval**
δ_{ij}	**Kronecker**
κ	**Turbulent Kinetic Energy**
ω	**Specific Dissipation**
Γ	**Turbulent thermal diffusivity**
η	**Coefficient** $(= \beta_R T_R)$
Θ	**Non-dimensional mean temperature**
θ	**Non-dimensional fluctuating temperature**
λ	**Thermal conductivity**
μ	**Dynamic viscosity**
v	**The Kinetic viscosity** $(= \mu/\rho_0)$
ρ	**Density**

σ_T	**Turbulent Prandtl number in Θ**
σ_κ	**Turbulent Prandtl in κ**
σ_ω	**Turbulent Prandtl in ω**
τ	**Viscous stress tensor**
π	**Stress tensor**
Φ	**Dissipation function**
ϕ	**General variable**
φ	**The instantaneous fluid property**

SUPER SCRIPT

b	**Boundary value**
c	**Cold wall**
h	**Hot wall**
i, j, k	**The i – th, j – th, k – th mesh point**
o	**Reference state**

SUB SCRIPTS

$n-1$	**Previous time step**
n	**Current time step**
$n+1$	**Next time step**
$'$	**Fluctuation quantity**
$*$	**Guessed value**

ABBREVIATIONS AND ACRONYMS

ADI	**Alternating Directional Implicit**
CFD	**Computational Fluid Dynamics**
CPU	**Central Processing Unit**
DNS	**Direct Numerical Simulation**
Eq.	**Equation**
FDM	**Finite Difference Method**
Fig.	**Figure**
FVM	**Finite Volume Method**
LES	**Large Eddy Simulation**
MADP	**Mean Absolute Deviation Percentage**
MHD	**Magneto-Hydrodynamic**
PISO	**Pressure Implicit Splitting Operator Algorithm**
RANS	**Reynolds Average Navier Stoke Equation**
SIMPLE	**Semi Implicit Method For Pressure Lined Equation**
SIMPLEC	**SIMPLE-Consistent**
SST	**Shear Stress Transport**
FLUENT	**Modelling Software**
LBM	**Lattice Boltzmann Method**
PDEs	**Partial Differential Equations**

CHAPTER ONE

INTRODUCTION

1.1 Background

Fluid mechanics deals with changes and behavior of a material. A fluid flows if a small force is applied and as a result there will be acceleration.

In an **incompressible fluid flow**, its density remains the same over the flow path while in a **compressible flow** its density depends on temperature and pressures in the flow field. In a **laminar flow**, fluids move on a smooth path and hence do not interfere with each other while a **turbulent flow** is a flow that is characterized by irregular flow and occurs in situations where the fluid's velocity is high. There are whirlpools in a turbulent flow. A **steady flow** is one in which the fluid properties such as velocity, pressure, temperature, and density are independent of time while in an **unsteady flow** the fluid properties are functions of time. Specifically, this study will be based on turbulent flow. The flow of heat moves from the object with the higher temperature to the one with a lower temperature.

Convection is an efficient way movement of fluids takes place when differences in temperatures in varying areas of the fluid is considered. Precisely, convection occurs when cooler fluids occupy the place for the warmer fluid resulting in a continuous circulation of fluids. In **radiation**, the flow of heat does not depend on the availability of any contact between the objects or fluid for heat to be transferred. This study will mainly be concerned with movement of heat through convection. In a natural convection, the occurrence of motion of a fluid results from the gravitational field that occurs due to differences in density resulting from varying temperatures.

Along these lines, there will be buoyant force causing dense fluid parts to move to the lower region while the less dense fluid parts will move upwards.

The movement of fluid in an enclosure caused by a difference in fluid density is known as **natural convection**. These differences may be caused by temperature, concentration, or decomposition gradients. Natural convection in an enclosure is complicated by the fluid's relationships with the borders. At the same time the complexity of this phenomenon is linked to our relative inability in determining interactions in an enclosure, therefore convections occurs due to orientations and surface geometry, temperature changes and velocity distributions. When convections occurs naturally, the movement of fluid is as a result of buoyancy and thus low velocity and low heat movement in the fluid.

When studying naturally occurring convective flows, the Rayleigh number is very important because it indicates the strength of the buoyancy force that maintains the equilibrium of the fluid flow. The force is due to density variation associated with temperature gradient within the flow domain. The Rayleigh number is thus a function of the thermal conditions of the confining walls .The non-dimensionless number incorporates the properties of the fluid and flow conditions into single parameters. For $Ra \leq 10^4$, movement of heat mechanics is mainly conduction while $10^4 \leq Ra \leq 10^9$, heat transfer is predominantly by laminar natural convection. For$Ra \gg 10^9$ movement of heat is turbulent.The fluid flows that are used in technical and industrial areas are of high viscosity that is the reason why we find turbulent flows in engineering applications.

1.2 Statement of the Problem

Previous research has been conducted on simulating turbulent natural convection fluid flow in an enclosure. Most researchers used vorticity-vector potential formulation to eliminate the pressure term in momentum equation. The current study simulates natural convections with primitive variables that is, to be able to solve for pressure gradient which is in the momentum equation using the PISO Method.

1.3 General Objective

To simulate natural turbulent convection in an enclosure using two equation $k-\omega$ turbulence Model and PISO method.

1.3.1 Specific Objectives

1. To simulate data for $k-\omega$ model for the velocity and temperature inside the enclosure.
2. To determine the effects of varying the Rayleigh number on the velocity and temperature distribution.
3. To determine change in velocity profiles, temperature profiles, convergence time, stability and accuracy when PISO method is used to solve for pressure term.

1.4 Significance of the study

This study will be applicable to various engineering practices. As such, the model can be used for saving on the computing requirements that could be needed for the solution of large turbulent flows. In addition, the results from this study could be used in the determination and control of micro-climate by ventilation, heating, and/or cooling of thermal comfort in a poultry house. Furthermore, the data from this study could be applied in the determination of optimum temperatures and/or velocity in a manufacturing plant for effective storage and preservation.

CHAPTER TWO

LITERATURE REVIEW

The naturally occurring convections that are turbulent finds applications in different engineering fields and attracts many researchers due to its importance. This study investigates numerical simulation of naturally occurring turbulent convections. Many studies have been done on natural convection in an enclosure.

Awuor (2012) investigated the performance of three numerical models namely *k-ε*, *k-ω* and *k-ω* SST with the aim of ascertaining the better approximation of experimental data in the process of predicting heat transfer profiles in an air-filled cavity. In the study, the author used Vorticity vector formulation in solving the momentum equation. It was noted that *k-ε* was not an effective model in the case where the temperature gradient at the boundaries is high but is useful in the free stream flows. In addition, it was deduced that *k-ω* SST model gives accurate predictions under adverse pressure gradient and accounts for the transport shear stress. In terms of the convergence time, he found that *k-ω* SST model is a more accurate model to be used in layer Simulation at a high temperature gradient in comparison to *k-ε* model and *k-ω* model. He further obtained numerical data using *k-ω* SST model

Edward *et al.* (2013) undertook a study on naturally occurring turbulent flow with a 3- dimensional boundary that had heaters on opposite sides of two windows placed opposite to each other. The velocity profile and the temperature distribution results in the room were presented in graphs. The governing equations of Newtonian fluid and the boundary conditions are discretized using three-point central difference approximation for the non-uniform mesh. The authors noted that the room is divided into numerous regions with the regions close to the heaters having higher temperatures as compared to the regions near the windows.

Goodarzi *et al.* (2014) have also investigated the effectiveness and accuracy of numerical method for simulation of natural convection heat transfer. The discretization of the LBM equations is done using the finite difference method. FLUENT was used for comparison purpose in the simulation of the problem. The results derived from the model were compared with the experimental data. It was noted that less CPU usage time is required for the cases of using finite volume methods in comparison with LBM. Furthermore, the authors espoused that there is a faster convergence and higher accuracy when using a combination of the first order upwind and SIMPLEC. The convergence of the FVM discretization and pressure velocity linking methods converged after a closely similar number of iterations.

Zimmerman and Groll (2014) undertook a numerical study in naturally occurring convections with huge turbulations. In the study, the acceleration in natural convection is driven by the differences in local densities and pressure gradient. The increase in temperature gradients is used in determining the temperature distribution in the heated walls. In the numerical model, they considered the change in density to occur due to change in temperature difference. The author made a comparison of the numerical results with the data from an experimental setup. It was noted that the temperature and the velocity showed an asymmetry as a result of effects on fluid non-Boussinesq. In the study, a recommendation for the study of an incompressible turbulent model simulation is made.

Wu and Lei (2015) studied turbulent natural convection in 2D and 3D with and without radiation transfer in heater cavities. Various Reynolds Average Navier- Strokes (RANS) turbulence model and the Discrete Ordinates radiation model were used in the numerical investigation. Further, Wu and Lei (2015) used quantitative and qualitative data for demonstration of the effects of three-dimensionality, thermal buoyancy condition and radiation transfer in surfaces that are horizontal.

Sajjadi and Kefayati (2015) carried out the Boltzmann mesh simulation with huge eddy simulations on turbulence natural convection in high enclosures that are filled with Air (Pr= 0.71) High Rayleigh numbers ranging from $10^7$and $10^9$and an aspect ratio between 0.5 and 2 were used in performing the calculations. The authors concluded that the average Nusselt number increases with the augmentation of Rayleigh numbers leading to a declination in the heat transfer in varying aspect ratios. The spectral-element method with high polynomial order was used to solve the unsteady time average governing equations. The results show the effect of the Rayleigh number on the local Nusselt number on the cold enclosure walls and the centrally located hot cylinder. According to the findings, the average and peak Nusselt numbers nearly double for each order of magnitude increase in the Rayleigh number for all radii. They also show how the average Nusselt number and Rayleigh and aspect ratio are related (Aithal 2016).

Kimunguyi (2016) undertook a computational investigation in natural turbulent convective flow using primitive variables in the solution of the time average equations governing the flow instead of making use of the vorticity- vector potential formulation. In this study, he carried out a non-dimensionalisation of the governing equations, the non- dimensional equations were then discretized using FVM and PISO and SIMPLEC algorithms were involved in the solution of these equations. The results of the study indicated that PISO method helps in the improvement of convergence time and speed. The method as well reduced the computational effort and there is a faster removal of the absolute error in the solution of flow. The author concluded that the obtained velocity profiles and temperature profiles were vital for use in ventilation systems for instance in the process of modelling of the flow of air in a room.

Josephs *et al* (2018) carried out a numerical investigation of Turbulent Natural convection in 3-D enclosure using $k-\omega \quad SST$ Model and SIMPLEC Method. The average statistical procedure of

mass, dynamics and energy governing equations adds unknown twisting correlations in the mean flow equations representing a turbulent transport of dynamic, heat and mass models by means of $k-\omega \quad SST$ model. They find that the non-dimensional temperature 0.5 at the cabin center and almost null at cold and the natural turbulent flow was responsible for the temperature distribution, both experimental data and the simulation using SIMPLEC.

In the current study we are investigating the simulation of natural convections with primitive variables in solving the pressure gradient which is in the momentum equation. The governing equations, turbulence, non-dimensionalisation and methodology for this particular numerical investigation of air is discussed in chapter three.

CHAPTER THREE

MATHEMATICAL FORMULATION

3.1 Governing Equations

3.1.1 Introduction

This Chapter discusses governing equations, turbulence, non-dimensionalisation and methodology for this numerical investigation of air in a 3-D enclosure.

The equations that govern the flow of an incompressible Newtonian fluid are deduced from equations that impose mass, velocity, and energy conservation. Equations governing natural convection in turbulent flow are represented by partial differential equations. These equations are then decomposed by expressing fluid properties as the sum of a mean and a fluctuating value.

3.1.2 Equation of Continuity

The law of conservation of mass is used in this equation. The rate of mass rise within a controlled volume is equal to the net rate of influx through the controlled surface, according to the law. The general equation of continuity in Cartesian tensor notation according to Curie (1974) is;

$$\frac{\partial \rho}{\partial t} + \frac{\partial}{\partial x_j}\left(\rho u_j\right) = 0 \tag{3.1}$$

Where j is 1,2,3,…

For steady state, equation (3.1) reduces to;

$$\frac{\partial}{\partial x_j}\left(\rho u_j\right) = 0 \tag{3.2}$$

This equation expresses the fact that, as fluid flows, matter is neither created nor destroyed and that mass is conserved. The equation is applicable to any type of flow, compressible or incompressible.

3.1.3 The Momentum Equation

The sum of forces acting on a control volume must equal the rate of rise in fluid speed within the control volume, according to Newton's second law of motion. In differential form, the Navier-Stokes equations can be expressed as;

$$\frac{\partial}{\partial t}\rho u_i + \frac{\partial}{\partial x_j}\rho u_i u_j = \rho F_i + \frac{\partial}{\partial x_j}(\pi_{ij}) \tag{3.3}$$

Where ρF_i represents the body force per unit volume and π_{ij} is the stress tensor, which for a Newtonian, according to White (1974), can be decomposed to;

$$\pi_{ij} = -P\delta_{ij} + \tau_{ij} \tag{3.4}$$

in which δ_{ij} is the Kronecker delta and τ_{ij} is the viscous stress tensor, which is given by;

$$\tau_{ij} = \mu\left(\frac{\partial u_i}{\partial x_j} + \frac{\partial u_j}{\partial x_i}\right) + \mu_s \delta_{ij}\frac{\partial u_k}{\partial x_k} \tag{3.5}$$

Where μ and $\mu_s$are the first and second coefficient of viscosity respectively. Therefore;

$$\tau_{ij} = -P\delta_{ij} + \mu\left(\frac{\partial u_i}{\partial x_j} + \frac{\partial u_j}{\partial x_i}\right) + \mu_s \delta_{ij}\frac{\partial u_k}{\partial x_k} \tag{3.6}$$

Electromagnetic forces are not considered in this work and the force of gravity is the only body force. Hence, in equation (3.3), putting $F_i = g_i$ where g_i is the force due to gravity in the x_i direction. Substituting equation (3.6) into (3.3) yields the momentum equation;

$$\frac{\partial}{\partial t}\rho u_i + \frac{\partial}{\partial x_j}\rho u_i u_j = -\frac{\partial P}{\partial x_i} + \rho g_i + \frac{\partial}{\partial x_j}\left[\mu\left(\frac{\partial u_i}{\partial x_j} + \frac{\partial u_j}{\partial x_i}\right) + \mu_s \delta_{ij}\frac{\partial u_k}{\partial x_k}\right] \tag{3.7}$$

3.1.4 The Energy Equation

The first law of thermodynamics is used to obtain the energy equation. It states that the rate of energy rise in a system is equal to the sum of the heat added to the system and the work performed on it and is often written according to Curie (1974) as;

$$\rho \frac{Dh}{Dt} + \frac{\partial}{\partial x_j}\left(\rho u_j \mathrm{h}\right) = \frac{\partial \rho}{\partial t} + \frac{\partial}{\partial x_j}\left(u_j \mathrm{p}\right) - \frac{\partial q_i}{\partial x_j} + \Phi \tag{3.8}$$

Where;

$$\Phi = \tau_{ij} \frac{\partial u_i}{\partial x_j} \tag{3.9}$$

is the dissipation function, h is the specific enthalpy and q_j is the local rate of heat transfer per unit area. In equation (3.9), the heat produced by the external forces has been neglected. The heat is modeled by Fourier's law, namely;

$$q_j = -\lambda \frac{\partial T}{\partial x_j} \tag{3.10}$$

in which λ is the thermal conductivity. Equation (3.8) can be simplified using the definition for specific enthalpy given as;

$$h = e + p/\rho \tag{3.11}$$

Where e is the specific internal energy. In differential form, equation (3.11) becomes;

$$\mathrm{d}h = \mathrm{d}e + p\mathrm{d}(1/\rho) \tag{3.12}$$

Using the first and the second law of thermodynamics (Hatsopolous and Keenan, 1965), the change in specific enthalpy can be expressed as;

$$\mathrm{d}e = T\mathrm{d}s - p\mathrm{d}(1/\rho) \tag{3.13}$$

Where s is the entropy. Substituting equation (3.13) into equation (3.12) yields;

$$\mathrm{d}h = T\mathrm{d}s + 1/\rho\, dp \tag{3.14}$$

Because entropy depends on the pressure and temperature, it can be written as; $s = s(T, P)$

$$\mathrm{d}s = \left(\frac{\partial s}{\partial p}\right)_T \mathrm{d}P + \left(\frac{\partial s}{\partial p}\right)_p \mathrm{d}T \tag{3.15}$$

and using the general thermodynamic relations (Hatsopolous and Keenan, 1965);

$$\left(\frac{\partial s}{\partial p}\right)_T = -\frac{\beta}{p}, \quad \left(\frac{\partial s}{\partial p}\right)_p = \frac{C_P}{T}, \quad \left(\frac{\partial \left[\frac{1}{\rho}\right]}{\partial T}\right)_T = -\frac{\beta}{p}$$

Hence equation (3.15) simplifies to;

$$\mathrm{d}s = -\frac{\beta}{p}\mathrm{d}P + \frac{C_P}{T}\mathrm{d}T \tag{3.16}$$

in which β is the volumetric coefficient of expansion and C_P is the specific heat at constant pressure. Substituting equation (3.16) into equation (3.14) results to;

$$\mathrm{d}h = C_P\mathrm{d}T + \frac{1}{\rho}(1 - \beta T)dp \tag{3.17}$$

substituting equations (3.17) and (3.10) into equation (3.8) makes the final form of the energy equation to be;

$$\frac{\partial}{\partial t}(C_P\rho T) + \frac{\partial}{\partial x_j}\left(C_P\rho u_j T\right) = \frac{\partial}{\partial x_j}\left(\lambda\frac{\partial T}{\partial x_j}\right) + \beta T\left(\frac{\partial p}{\partial t} + \frac{\partial u_j p}{\partial x_j}\right) + \Phi \tag{3.18}$$

Equations (3.1), (3.7), (3.18) and the equation of state relating the local density to the local values of temperature and pressure, coupled with appropriate boundary conditions discussed in section

3.10, can be used to determine the velocity component u_j and fluid properties ρ, p and T in both laminar and turbulent flow.

3.2 Turbulence Modelling

3.2.1 Reynolds Decomposition

Exact modeling of turbulent flow requires the exact solution of the Continuity and Navier-Stokes equations which can be extremely difficult and time consuming due to the many scales involved. To reduce the complexity, an approximation to the Navier-Stokes equation was developed by Osborne Reynolds (1894) called the Reynolds-averaged Navier-Stokes equations (or RANS equations). The concept entails decomposing the instantaneous fluid flow quantities in the Navier-Stokes equations into mean value and fluctuating value.

Modeling of turbulence is based on the concept that fluid properties at a given point exhibit a net mean behavior with small fluctuations about it as a function of time. The instantaneous fluid property φ as a function of time t is, at a given point is shown in figure 3.1 below where an arbitrary flow property φ is shown at some location in the flow:

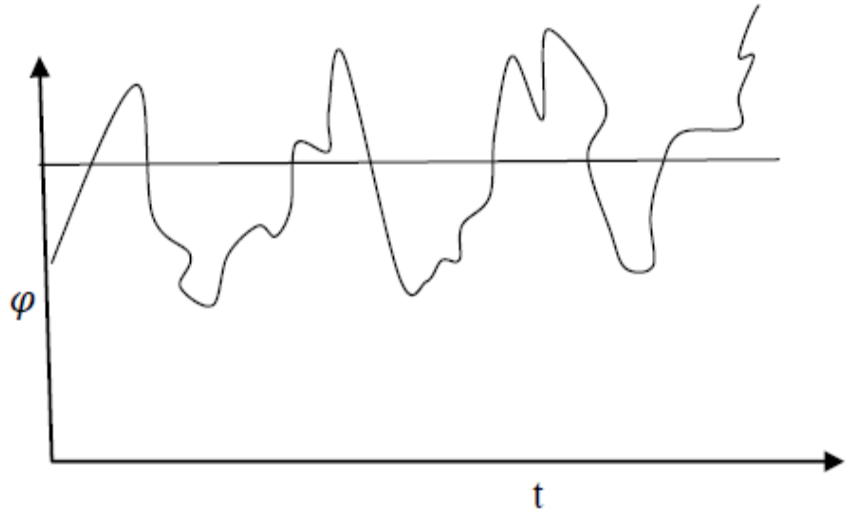

Figure 3.1 Fluid property of turbulence as a function of time t

The property φ is the instantaneous quantity which could be a velocity components, pressure component, fluid temperature or any other fluid property. We define the time average variable $\bar{\varphi}$ as;

$$\bar{\varphi} \equiv \frac{1}{T_1}\int_0^{T_1} \varphi dt \tag{3.19}$$

Where T_1 is a time large enough such that $\bar{\varphi}$ is the same for any larger time for a steady mean flow. The overbar denotes the time average ofφ. The instantaneous quantity φ may be written in terms of a time average $\bar{\varphi}$ and a fluctuating quantity, as;

$$\varphi = \bar{\varphi} + \varphi' \tag{3.20}$$

Similarly, for scalar quantities;

$$\emptyset = \overline{\emptyset} + \emptyset' \tag{3.21}$$

Where $\emptyset'$denotes a scalar such as temperature, energy, pressure or turbulent quantities.

3.2.2 Instantaneous Equations of Motion

A turbulent flow instantaneously satisfies the Navier-Stokes equations. The method of developing these equations of motion involves, first writing the equations for the instantaneous quantities. Then we take the time average of both sides, noting that if the quantity is valid instantaneously then it is also valid on the average for some period of time. Finally we simplify the equations such that only the average quantities appear. We take the assumption that the variation of densities are caused by fluctuations of temperature. Under the Boussinesq (1903) approximation, the equations of motion for the instantaneous variables are found from equations (3.1), (3.7) and (3.18) which become;

$$\frac{\partial \tilde{\rho}}{\partial t} + \frac{\partial}{\partial x_i}\left(\tilde{\rho}\tilde{u}_j\right) = 0 \tag{3.22}$$

$$\frac{\partial}{\partial t}\tilde{\rho}\tilde{u}_j + \frac{\partial}{\partial x_j}\tilde{\rho}\tilde{u}_i\tilde{u}_j = -\frac{\partial \tilde{P}}{\partial x_i} + \tilde{\rho}g_i + \frac{\partial}{\partial x_j}\left[\mu\left(\frac{\partial \tilde{u}_i}{\partial x_j} + \frac{\partial \tilde{u}_j}{\partial x_i}\right) + \mu_s\delta_{ij}\rho\frac{\partial \tilde{u}_j}{\partial x_k}\right] \tag{3.23}$$

$$\frac{\partial}{\partial t}\left(\tilde{C}_P\tilde{\rho}\tilde{T}\right) + \frac{\partial}{\partial x_j}\left(\tilde{C}_P\tilde{\rho}\tilde{U}_j\tilde{T}\right) = \frac{\partial}{\partial x_j}\left(\lambda\frac{\partial \tilde{T}}{\partial x_j}\right) + \beta T\left(\frac{\partial \tilde{p}}{\partial t} + \frac{\partial \tilde{u}_j\tilde{p}}{\partial x_j}\right) + \Phi \tag{3.24}$$

The mean flow equations are obtained by substituting the Reynolds decomposition to the instantaneous continuity equation (3.22), momentum equation (3.23) and energy equation and taking the average of the equations. From equation (3.22), we decompose the variable $\tilde{u}_j$ and $\tilde{\rho}$

into time average variables plus fluctuating components as given by equation (3.20). That is $\tilde{\rho} = \bar{\rho} + \rho', \bar{u}_j + u_j'$.

3.2.3 Averaged Equations of Motion

a) Continuity equation for Turbulent flow

This equation is valid for turbulent flow, and the dependent variables represent instantaneous quantities. Decomposing instantaneous continuity equation into its mean and turbulent part yields;

$$\frac{\partial}{\partial t}(\bar{\rho} + \rho') + \frac{\partial}{\partial x_j}(\bar{\rho} + \rho')\left(\bar{u}_j + u_j'\right) = 0 \tag{3.25}$$

Time averaging the entire equation gives;

$$\overline{\frac{\partial}{\partial t}(\bar{\rho} + \rho') + \frac{\partial}{\partial x_j}(\bar{\rho} + \rho')\left(\bar{u}_j + u_j'\right)} = \overline{\frac{\partial}{\partial t}(\bar{\rho} + \rho')} + \overline{\frac{\partial}{\partial x_j}(\bar{\rho} + \rho')\left(\bar{u}_j + u_j'\right)} = 0$$

Where

$$\overline{\frac{\partial}{\partial t}(\bar{\rho} + \rho')} = \frac{\partial \overline{\bar{\rho} + \rho'}}{\partial t} = \frac{\partial \bar{\rho}}{\partial t} + \frac{\partial \overline{\rho'}}{\partial t} = \frac{\partial \bar{\rho}}{\partial t}$$

Because;

$$\frac{\partial \overline{\rho'}}{\partial t} = 0$$

$$\overline{\frac{\partial}{\partial x_j}(\bar{\rho} + \rho')\left(\bar{u}_j + u_j'\right)} = \overline{\frac{\partial}{\partial t}\left(\bar{\rho}\bar{u}_j + \bar{\rho}u_j' + \rho'\bar{u}_j + \rho' u_j'\right)}$$

Taking the time average, expanding and simplifying equation (3.28), we obtain;

$$\frac{\partial}{\partial x_j}\left(\bar{\rho}\bar{u}_j + \bar{\rho}\overline{u_j'} + \overline{\rho'}\bar{u}_j + \overline{\rho' u_j'}\right) = \frac{\partial}{\partial x_j}\left(\bar{\rho}\bar{u}_j + \overline{\rho' u_j'}\right) \; since \; \overline{u_j'} = \overline{\rho'} = 0$$

Given that the terms which are linear in fluctuating quantities become zero when time averaged. Therefore the time averaged continuity equation becomes;

$$\frac{\partial \bar{\rho}}{\partial t} + \frac{\partial}{\partial x_j}\left(\bar{\rho}\bar{u}_j + \overline{\rho' u_j'}\right) = 0 \tag{3.26}$$

b) Momentum Equation for Turbulent Flow

Decomposing the instantaneous dependent variables of the momentum equation (3.23) into their mean and fluctuating parts yields;

$$\frac{\partial}{\partial t}(\bar{\rho} + \rho')\left(\bar{u}_j + u_j'\right) + \frac{\partial}{\partial x_j}(\bar{\rho} + \rho')(\bar{u}_i + u_i')\left(\bar{u}_j + u_j'\right)$$

$$= -\frac{\partial(\bar{P} + P')}{\partial x_i} + (\bar{\rho} + \rho')g_j + \frac{\partial}{\partial x_j}\left[\mu\left(\frac{\partial(\bar{u}_i + u_i')}{\partial x_j} + \frac{\left(\bar{u}_j + u_j'\right)}{\partial x_i}\right) + \mu_s \delta_{ij}\rho\frac{\partial(\bar{u}_k + u_k')}{\partial x_k}\right]$$

Averaging each term on both sides;

$$\overline{\frac{\partial}{\partial t}(\bar{\rho} + \rho')\left(\bar{u}_j + u_j'\right)} = \overline{\frac{\partial}{\partial x_j}\left(\bar{\rho}\bar{u}_j + \bar{\rho}\overline{u_j'} + \overline{\rho'}\bar{u}_j + \rho' u_j'\right)} + \frac{\partial}{\partial t}\left(\bar{\rho}\bar{u}_j + \bar{\rho}\overline{u_j'} + \overline{\rho'}\bar{u}_j + \overline{\rho' u_j'}\right)$$

$$= \frac{\partial}{\partial x_j}\left(\bar{\rho}\bar{u}_j + \overline{\rho' u_j'}\right)$$

$$\overline{\frac{\partial}{\partial x_j}(\bar{\rho} + \rho')(\bar{u}_\iota + u_\iota')\left(\bar{u}_j + u_j'\right)} = \frac{\partial}{\partial x_j}\overline{(\bar{\rho} + \rho')(\bar{u}_\iota + u_\iota')\left(\bar{u}_j + u_j'\right)}$$

Where;

$$(\bar{\rho} + \rho')(\bar{u}_i + u_i')\left(\bar{u}_j + u_j'\right) = \left(\bar{\rho}\bar{u}_j + \bar{\rho}u_j' + \rho'\bar{u}_j + \rho' u_j'\right)\left(\bar{u}_j + u_j'\right)$$

$$= \bar{\rho}\bar{u}_j\bar{u}_j + \bar{\rho}\bar{u}_j u_j' + \bar{\rho}u_j'\bar{u}_j + \bar{\rho}u_j'u_j' + \rho'\bar{u}_j\bar{u}_j + \rho'\bar{u}_j u_j' + \rho' u_j'\bar{u}_j + \rho' u_j' u_j'$$

And;

$$\overline{(\bar{\rho}+\rho')(\bar{u}_\iota + u_\iota')\left(\bar{u}_\jmath + u_\jmath'\right)} = \bar{\rho}\bar{u}_j\bar{u}_j + \bar{\rho}\overline{u_j'u_j'} + \bar{\rho}'\bar{u}_j\bar{u_j'} + \overline{\rho' u_j'}\bar{u}_j + \overline{\rho' u_j' u_j'}$$

So that;

$$\frac{\partial}{\partial x_j}\overline{\left((\bar{\rho}+\rho')(\bar{u}_\iota + u_\iota')\left(\bar{u}_\jmath + u_\jmath'\right)\right)} = \frac{\partial}{\partial x_j}\left(\bar{\rho}\bar{u}_j\bar{u}_j + \bar{\rho}\overline{u_j'u_j'} + \bar{\rho}'\bar{u}_j\bar{u_j'} + \overline{\rho' u_j'}\bar{u}_j + \overline{\rho' u_j' u_j'}\right)$$

$$\frac{\partial}{\partial x_j} = \left(\bar{\rho}\bar{u}_j\bar{u}_j + \bar{\rho}'\bar{u}_i\bar{u}_j\right)$$

And;

$$\overline{\frac{\partial(\bar{P}+P')}{\partial x_\iota}} = \frac{\overline{\partial(\bar{P}+P')}}{\partial x_\iota} = \frac{\partial\left(\bar{P}+P'\right)}{\partial x_i} = \frac{\partial(\bar{P})}{\partial x_i}$$

$$\overline{(\bar{\rho}+\rho')}g_j = (\bar{\rho}+\rho')g_j = \bar{\rho}g_j$$

Therefore;

$$\overline{\frac{\partial}{\partial x_\jmath}\left[\mu\left(\frac{\partial(\bar{u}_\iota + u_\iota')}{\partial x_\jmath} + \frac{\left(\bar{u}_\jmath + u_\jmath'\right)}{\partial x_\iota}\right) + \mu_s\delta_{\iota\jmath}\rho\frac{\partial(\bar{u}_k + u_k')}{\partial x_k}\right]} = \frac{\partial}{\partial x_j}\left[\mu\left(\frac{\partial\bar{u}_i}{\partial x_j} + \frac{\partial\bar{u}_j}{\partial x_i}\right) + \mu_s\delta_{ij}\frac{\partial\bar{u}_k}{\partial x_k}\right]$$

Therefore, the Reynolds form of the equation becomes;

$$\frac{\partial}{\partial t}\left(\bar{\rho}\bar{u}_j + \overline{\rho' u_j'}\right) + \frac{\partial}{\partial x_j}\left(\bar{\rho}\bar{u}_j\bar{u}_j + \bar{\rho}'\bar{u}_i\bar{u}_j\right) = -\frac{\partial(\bar{P})}{\partial x_i} + \bar{\rho}g_j + \frac{\partial}{\partial x_j}\left(\bar{\tau}_{ij} - \bar{u}_j\overline{\rho' u_j'} - \overline{\rho u_\iota' u_j'} - \overline{\rho' u_\iota' u_j'}\right) \quad (3.27)$$

In which;

$$\tau_{ij} = \mu\left(\frac{\partial \bar{u}_i}{\partial x_j} + \frac{\partial \bar{u}_j}{\partial x_i}\right) + \mu_s \delta_{ij} \frac{\partial \bar{u}_k}{\partial x_k} \tag{3.28}$$

c) Energy equation for Turbulent Flow

Similarly, the energy equation (3.24) can be decomposed using equation (3.21) and the resulting equation is time averaged and simplified by eliminating terms known to be zero to yield;

$$\frac{\partial}{\partial t}(C_P \bar{\rho}\bar{T} + C_P\overline{\rho' T'}) + \frac{\partial}{\partial x_j}\left(C_P \overline{\rho u_j}\bar{T}\right) = \frac{\partial \bar{p}}{\partial t} + \frac{\partial \bar{p}}{\partial x_j} + \overline{u_i' \frac{\partial p'}{\partial x_j}} + \frac{\partial}{\partial x_j}\left(\lambda \frac{\partial \bar{T}}{\partial x_j} - C_P \bar{\rho}\overline{u_i' T'} - C_P \overline{\rho' u_i T'}\right) + \bar{\Phi} \tag{3.29}$$

Where;

$$\bar{\Phi} = \overline{\tau_{ij}} \frac{\partial \bar{u}_i}{\partial x_j} + \overline{\tau_{ij}' \frac{\partial u_i'}{\partial x_j}} \tag{3.30}$$

The τ_{ij} in the equation (3.30) should be evaluated as expressed in equation (3.28).

The mean continuity and momentum equations adds unknown quantities which represent the mean effect turbulence. These terms enter the governing equations as turbulent transport terms, such as $\overline{\rho' u_i' u_j'}$ and density generated terms as $\overline{\rho' u_j'}$ and $\overline{\rho' u_i'}$. In the mean energy equation, the time averaging process introduces unknown turbulent correlation between temperature fluctuation $\overline{u_i' T'}$ or $\overline{u_j' T'}$ which, when multiplied by density ρ, they represent transport of heat or mass due to fluctuation motion. The term $-\overline{\rho u_i' T'}$ is the transport in the direction x_i or rather the turbulent heat flux. Mass weighted averages eliminate the mean mass term $\overline{\rho' u_j'}$ and some momentum transport terms such as $\overline{\rho' u_i' u_j'}$ across mean streamline (Cebeci and Smith, 1974).

Equations (3.26), (3.27) and (3.29) are equations generally accepted as governing the mean flow quantities $\bar{u}_i$ and fluid properties $\bar{\rho}, \bar{p}$ and temperature $\bar{T}$.

3.3 Reynolds Stress Equations

Let us refer to the time averaged continuity equation (3.26) and Navier-Stokes equation (3.27), in which upper and lower case of letters would be used to refer to mean and fluctuating quantities for the case of velocity components, written in Cartesian tensor below;

$$\mu \frac{\partial P}{\partial t} + (\rho \overline{U}_i)_{,} i = 0 \tag{3.31}$$

$$\frac{\partial \rho \overline{U}_i}{\partial t} + \left(\rho \overline{U}_i \overline{U}_j\right)_{,} j = -\bar{P}_{,} i + \left[\mu\left(\overline{U}_{i,j} + \overline{U}_{j,i}\right) - \rho \overline{u_i u_j}\right]_{,} j \tag{3.32}$$

3.3.1 Boussinesq Assumption

The turbulent viscosity is used in eddy viscosity turbulence models to link the Reynolds stresses to the velocity gradients (i.e., the eddy viscosity principle assumes a similarity between molecular motions, which leads to Stoke's viscosity law in laminar flow, and instantaneous turbulent motion). The Reynolds stress tensor in the time averaged Navier-Stokes equation (3.32) is replaced by the turbulent viscosity multiplied by the velocity gradients in the Boussinesq assumption.

This is demonstrated by introducing this assumption for the diffusion term on the right-hand side of Equation (3.32) and making an identification;

$$\left[\mu\left(\overline{U}_{i,j} + \overline{U}_{j,i}\right) - \rho \overline{u_i u_j}\right]_{,} j = \left[(\mu + \mu_t)\left(\overline{U}_{i,j} + \overline{U}_{j,i}\right)\right]_{,} j \tag{3.33}$$

Equation (3.33) on expansion and re-arrangement gives;

$$\rho \overline{u_i u_j} = -\mu\left(\overline{U}_{i,j} + \overline{U}_{j,i}\right) \tag{3.34}$$

If we do a contraction in equation (3.34) (i.e. Setting *i=j*) the right-hand side gives;

$$\overline{u_\iota u_j} \equiv 2k \tag{3.35}$$

Where The turbulent kinetic energy is denoted by k. Using the continuity equation (3.31), on the other hand, the right-hand side of the equation (3.34) is reduced to zero.

3.3.2 The Eddy Viscosity Concept – The closure Problem

To validate equation (3.34) upon contraction, we add $\frac{2}{3}\delta_{ij}\rho k$ to the right-hand side of equation (3.34) so that;

$$\rho\overline{u_\iota u_j} = -\mu_t\left(\overline{U}_{i,j} + \overline{U}_{j,i}\right) + \frac{2}{3}\delta_{ij}\rho k \tag{3.36}$$

Note that the contraction of δ_{ij} gives;

$$\delta_{ii} = \delta_{11} + \delta_{22} + \delta_{33} \tag{3.37}$$

Equation (3.36) can likewise be written as;

$$\tau_{ij} = -\overline{\rho u_i' u_\iota'} = \mu_t\left(\frac{\partial\overline{u}_i}{\partial x_j} + \frac{\partial\overline{u}_i}{\partial x_j}\right) + \frac{2}{3}\bar{\rho}k\delta_{ij} \tag{3.38}$$

Where:

- μ_t is the turbulent or eddy viscosity, the proportionality parameter that links the turbulent stresses and the mean flow velocity gradient (or the mean strain rate). Like molecular viscosity, its unit is Pascal seconds.
- Turbulent viscosity is not homogenous, i.e. it varies in space. It is however assumed to be isotropic.
- *k* is kinetic energy of the turbulent velocity fluctuations given by;

$$k = \frac{1}{2}\overline{u_i' u_\iota'} \tag{3.39}$$

This method was first postulated by Boussinesq (1903) and consequently denoted the Boussinesq hypothesis.

Further;

$$-\overline{\rho u_j' T'} = \frac{k_t}{C_P}\frac{\partial T}{\partial x_i} \tag{3.40}$$

k_t is the turbulent conduction coefficient. In contrast to molecular viscosity μ and thermal conductivity of the fluid λ in laminar flow, μ_t and k_t are not fluid properties but flow properties. The problem at the moment is to device means of solving the turbulent stress, τ_{ij} and the turbulent heat $\overline{\rho u_j' T'}$. In this study, a two-equation model, $\kappa - \omega$ SST model, is used to solve this problem. This is actually one of the most commonly used turbulence model. In this model, the idea is to express turbulence viscosity as a function of κ and ω and then derive PDEs of κ andω. Relationships for eddy viscosity μ_t and turbulent specific dissipation ω are required for closure.

The square root of the turbulent kinetic energy $\kappa^{\frac{1}{2}}$ can be used to represent a velocity scale for the large scale turbulent motion. Accordingly, the eddy viscosity is considered proportional to a velocity characterizing the fluctuating motion and to a typical length of this motion which Prandtl (1945) called; mixing length. Using this equation, an eddy viscosity relation yields;

$$\mu_t \propto \kappa^{\frac{1}{2}} l \tag{3.41}$$

$$\mu_t = C_\mu \kappa^{\frac{1}{2}} l \tag{3.42}$$

Where l the turbulent length is scale and C_μ is a constant which has to be determined empirically. From the definition of turbulent length scale;

$$l = \frac{\kappa^{\frac{1}{2}}}{\varepsilon} \tag{3.43}$$

Hence

$$\mu_t = C_\mu \kappa^{\frac{1}{2}} l = \mu_t = C_\mu \kappa^{\frac{1}{2}} \frac{\kappa^{\frac{1}{2}}}{\varepsilon} = C_\mu \frac{\kappa^2}{\varepsilon} \tag{3.44}$$

Where ε is turbulent dissipation.

The turbulent variable ω was defined by Wilcox (1998) as:

$$\omega = \frac{\varepsilon}{C_\mu \kappa} \tag{3.45}$$

Hence from equation (3.45) above, $\varepsilon = C_\mu \kappa \omega$

The eddy viscosity for the formulation, Wilcox (1998), using equation (3.44) where $\mu_t = C_\mu \frac{\kappa^2}{\varepsilon}$ is

$$\mu_t = \frac{\kappa}{\omega} \tag{3.46}$$

And

$$\kappa_t = \frac{\mu_t C_p}{P_r} \tag{3.47}$$

The model includes two transport equations to represent the turbulent properties of the flow. The first transport variable is the turbulent kinetic energyκ. The second transport variable is the specific dissipationω. It is the variable that determines the length scale the turbulence.

3.3.3 The Exact Kinetic Energy Equation

The equation for turbulent kinetic energy $k = \frac{1}{2}\overline{u_i' u_i'}$ is derived from the Navier-Stokes equation, assuming steady, incompressible constant viscosity, reads;

$$\left(\rho U_i U_j\right) j = -P_{,i} + \mu U_{i,jj.} \tag{3.48}$$

Where, *j* denotes derivation with respect to x_j.

The time averaged Navier-Stokes equation is;

$$\left(\rho \overline{U}_i \overline{U}_j\right) j = -\overline{P}_{,} i + \mu U_{i,jj} - \left(\rho \overline{u_\iota u_J}\right)_{,j} \tag{3.49}$$

Subtracting equation (3.49) from equation (3.48), multiplying by u_i and time averaging resultant equation yields;

$$\overline{\left[\rho U_\iota U_J - \rho \overline{U}_\iota \overline{U}_J\right]_{,J} u_\iota} = -\overline{[P - \bar{P}]_{,\iota} u_\iota} + \overline{\mu [U_\iota - \overline{U}_\iota]_{,JJ} u_\iota} + \rho \overline{\overline{u_\iota}\overline{u_J}]_{,J} u_\iota} \tag{3.50}$$

The left hand-side can be written as;

$$\overline{\rho\left[(\overline{U}_\iota + u_\iota)(\overline{U}_J + u_J) - \overline{U}_\iota \overline{U}_J\right]_{,J} u_\iota} = \overline{\rho\left[\overline{U}_\iota u_J + u_\iota \overline{U}_J + u_\iota u_J\right]_{,J} u_\iota} \tag{3.51}$$

Using the continuity equation, $\left(\rho \overline{U}_j\right)_{,j} = 0$, , the first term is re-written as;

$$\overline{\rho\left(\overline{U}_\iota u_J\right)_{,J} u_\iota} = \rho \overline{u_\iota u_J} \overline{U}_{i,j} \tag{3.52}$$

We obtain the second term $\left(\rho \overline{U}_j\right)_{,j} = 0$ from;

$$\overline{\left(\rho \overline{U}_J k\right)_{,J}} = \overline{U}_j \overline{\rho\left[\frac{1}{2} u_\iota u_J\right]_{,J}} = \frac{1}{2} \rho \overline{U}_j \overline{\left\{u_\iota u_{\iota,J} + u_\iota u_{\iota,J}\right\}_{,J} u_\iota} = \overline{u_\iota \left(\rho \overline{U}_\iota u_J\right)_{,J}} \tag{3.53}$$

Using the same technique as in equation (3.53) where $\overline{\left[\frac{1}{2}u_\iota u_\jmath\right]_{,\jmath}} = \frac{1}{2}\overline{\left\{u_\iota u_{\iota,\jmath} + u_\iota u_{\iota,\jmath}\right\}_{,\jmath} u_\iota}$, the third term in equation (3.51) can be written as;

$$\frac{1}{2}\overline{\left(\rho u_\jmath u_\iota u_\jmath\right)}_{,j} \tag{3.54}$$

The first term of equation (3.51) on the right-hand side has the form;

$$-\overline{P_{,\iota} u_\iota} = -\overline{(P u_\iota)}_{,j} \tag{3.55}$$

The second term on the right-hand side of equation (3.51) read;

$$\mu\overline{U_{\iota,\jmath\jmath} u_\iota} = \mu\left\{\overline{\left(u_{\iota,\jmath} u_\iota\right)_{,\jmath} - u_{\iota,\jmath} u_{\iota,\jmath}}\right\} \tag{3.56}$$

Using the approach as in equation (3.53),

$$\text{where } \overline{\left[\frac{1}{2}u_\iota u_\jmath\right]_{,\jmath}} = \frac{1}{2}\overline{\left\{u_\iota u_{\iota,\jmath} + u_\iota u_{\iota,\jmath}\right\}_{,\jmath} u_\iota} \tag{3.57}$$

the first term becomes;

$$\mu\overline{\left(u_{\iota,\jmath} u_\iota\right)}_{,j} = \mu\frac{1}{2}\overline{(u_\iota u_\iota)_{\jmath\jmath}} = \mu k_{jj} \tag{3.58}$$

The last term on the right-hand side of the equation (3.50) is zero.

We can now put together the transport equation for turbulent kinetic energy. Equations (3.52), (3.53), (3.55), (3.56), (3.57) give;

$$\underbrace{\left(\rho\overline{U}_\jmath k\right)_{,j}}_{\text{I}} = \underbrace{-\rho\overline{u_\iota u_\jmath}\overline{U}_{i,j}}_{\text{II}} - \underbrace{\left[\overline{u_\jmath P} + \frac{1}{2}\overline{\rho u_\jmath u_\iota u_\jmath} - \mu k_\jmath\right]_{,j}}_{\text{III}} - \underbrace{\mu\overline{\left(u_{\iota,\jmath} u_\iota\right)}_{,j}}_{\text{IV}} \tag{3.58}$$

The terms in equation (3.58) are:

I. Convection.

II. Production.

III. The three terms in this term are; turbulent diffusion by pressure-velocity fluctuations, velocity fluctuations and viscous diffusion in that order.

IV. Dissipation.

3.3.4 The Modeled k-Equation

The exact kinetic energy equation (3.58) has unknown terms.

Inserting equation (3.38) in the production term in equation (3.58) we have;

$$P_k = -\rho\overline{u_\iota u_j}\overline{U}_{i,j} = \mu_t\left(\overline{U}_{i,j} + \overline{U}_{j,i}\right)\overline{U}_{i,j} + \frac{2}{3}\delta_{ij}\rho k\overline{U}_{i,i} \tag{3.59}$$

For incompressible flow, the last term in equation (3.59) is zero due to continuity, as shown in equation (3.31).

i. A gradient law is used to model the triple correlations in term III of equation (3.58), where we assume that k is diffused down the gradient. This yields;

$$\frac{1}{2}\overline{\rho u_j u_\iota u_\iota} = \frac{\mu_t}{\sigma_k}k, j \tag{3.60}$$

Where σ_k is the turbulent Prandtl number. The pressure diffusion term in equation (3.58). is small and hence its negligible.

ii. The dissipation term in equation (3.58) is estimated as;

$$\varepsilon = O\frac{u^2}{l/u} = O\frac{u^3}{l} \tag{3.61}$$

where *O* is the order of the function

which is a relation for the cascade process and $\varepsilon = (m^2/s^3)$ is the energy per unit time per unit mass.

Therefore, as per equation (3.61), the velocity scale is now;

$$u = \sqrt{k} \tag{3.62}$$

Therefore;

$$\varepsilon = \sqrt{u_{i,j}u_{i,j}} = \frac{k^{\frac{3}{2}}}{l} v = \frac{\mu}{\rho} \tag{3.63}$$

Where $v = \frac{\mu}{\rho}$

Hence;

$$\mu\overline{u_{\iota,j}u_{\iota,j}} = \rho\varepsilon = \rho\frac{k^{\frac{3}{2}}}{l} \tag{3.64}$$

The modeled *k* equation can now be assembled to give;

$$\left(\rho\bar{U}_j k\right)_{,j} = \left(\mu + \frac{\mu_t}{\sigma_k}\right) k_{,j} + P_k - \rho\frac{k^{\frac{3}{2}}}{l} \tag{3.65}$$

An additional transport equation is required to compute *l*. In the $\kappa - \omega$ model, the length determining equation ω is used. This quantity is often called specific dissipation from its definition which is;

$$\omega = \frac{\varepsilon}{\kappa} \tag{3.66}$$

The modeled κ and ω equations are respectively;

$$\left(\rho U_j k\right)_{,j} = \left[\left(\mu + \frac{\mu_t}{\sigma_k}\right) k_{,j}\right]_{,j} + P_k - \beta^*\omega k \tag{3.67}$$

$$\left(\rho\bar{U}_j \omega\right)_{,j} = \left[\left(\mu + \frac{\mu_t}{\sigma_k}\right) \omega_{,j}\right]_{,j} + \frac{\omega}{k}\left(C_{w1}P_k - C_{w2}\rho k\omega\right) \tag{3.68}$$

Where;

$$\mu_t = \rho\frac{\kappa}{\omega} \tag{3.69}$$

$$\varepsilon = \beta^* \omega k \tag{3.70}$$

The constants are determined from experiments.

$k_{wall} = 0$ is the turbulent kinetic energy's wall boundary condition. Because the turbulent kinetic energy at the wall is zero, then the eddy viscosity is also zero at the wall. Hence from the definition of the specific dissipationω, ($\omega = \frac{\varepsilon}{C_\mu \kappa}$) it implies that ω should go to infinity at the wall since *k* tends to zero. Basing on asymptotic arguments, Wilcox (1998) suggested that it be given the value $\omega_{wall} = \frac{60v}{C_\mu(\Delta y^2)}$ at the wall where Δy is the normal distance to the first point off the wall. Free stream boundary conditions;

$$\frac{V_{t\infty}}{V_\infty} = 0.0001, \qquad \omega_\infty = 10\frac{U_\infty}{l} \qquad k_\infty = V_\infty \omega_\infty \tag{3.71}$$

3.4 Final Set of Equations

For simplicity, from thus point onwards, the over-bar indicating time mean values of the variables and the prime indicating the fluctuating quantities will be replaced by the upper and lower case letters respectively. The final set of equations for turbulent natural convection flows is:

$$\frac{\partial \rho}{\partial t} + \frac{\partial}{\partial x_j}\left(\rho U_j + \overline{\rho u_\iota}\right) = 0 \tag{3.72}$$

$$\frac{\partial}{\partial t}(\rho U_i + \overline{\rho u_\iota}) + \frac{\partial}{\partial x_j}\left(\rho U_i U_j + U_i \overline{\rho u_\iota}\right) = -\frac{\partial P}{\partial x_i} + p g_i + \frac{\partial}{\partial x_j}\left(\tau_{ij} - U_i \overline{\rho u_\iota} - \rho \overline{u_\iota u_J} - \overline{\rho u_\iota u_j}\right) \tag{3.73}$$

$$\frac{\partial}{\partial t}(C_P \rho T + C_P \overline{\rho T}) + \frac{\partial}{\partial x_j}\left(C_P \overline{\rho u_j T}\right) = \frac{\partial p}{\partial t} + U_j \frac{\partial p}{\partial x_j} + \overline{u_J \frac{\partial p}{\partial x_J}} + \frac{\partial}{\partial x_j}\left(\lambda \frac{\partial T}{\partial x_j} - C_P \overline{u_t T} - C_P \overline{u_\iota T}\right) + \Phi \tag{3.74}$$

Where;

$$\tau_{ij} = \mu\left(\frac{\partial U_i}{\partial x_j} + \frac{\partial U_j}{\partial x_i}\right) + \mu_s \delta_{ij} \frac{\partial u_k}{\partial x_k} \tag{3.75}$$

$$\Phi = \tau_{ij} + \frac{\partial U_i}{\partial x_j} + \overline{\mu\left(\frac{\partial u_\iota}{\partial x_\jmath} + \frac{\partial u_\jmath}{\partial x_\iota}\right)\frac{\partial u_\iota}{\partial x_\jmath}} \tag{3.75}$$

$$\frac{\partial}{\partial t}\rho k + \frac{\partial}{\partial x_j}\left((\rho U_i k)\right) = \overline{u_\jmath \frac{\partial}{\partial x_\jmath}\mu\frac{\partial u_\iota}{\partial x_\jmath}} + \overline{\frac{\partial u_\iota}{\partial x_\jmath}} - \frac{1}{2}\frac{\partial}{\partial x_j}\overline{\rho u_\iota u_\iota u_\jmath} - \rho\overline{u_\iota u_\jmath}\frac{\partial u_i}{\partial x_j} + \overline{\rho u_\iota} g_i - \overline{u_\jmath \frac{\partial p}{\partial x_\iota}}$$

(3.67)

$$\frac{\partial \omega}{\partial t} + U_i \frac{\partial \omega}{\partial x_j} = -\frac{\partial}{\partial x_i}\left[\left(\mu + \frac{\mu_t}{\sigma_\omega}\right)\frac{\partial \omega}{\partial x_j}\right] + \left[\beta - \frac{k^2}{\sigma_\omega\sqrt{c_u}}\right]\frac{\omega}{k}P_k - \beta\omega^2 \tag{3.77}$$

3.5 Non- Dimensionalisation

A suitable substitution of variable is used to remove units from an equation containing physical quantities, either partially or completely. This method can be used to simplify and parametize problems involving measured units. In fluid mechanics, the adoption of a suitable non-dimensional scheme is important, Jiyuan *et al.* (2012). An appropriate scheme does the following:-

i. It expresses experimental and analytical results in the most efficient form.

ii. Makes the solution bounded for instance, temperature can be non-dimensionalized such that it varies from 0 to 1.

All the dependent and independent flow variables can be derived by valid and significant constant quantities to obtain the non-dimensional form of the governing equations (and boundary conditions). All velocities U_* can be grouped by a reference velocity L_0 (which is the inlet velocity), pressure by $P_0 = \rho U_*^2$ (which is twice the dynamic pressure for the channel), and temperature by a suitable temperature difference (which is $\{T - T_*\}/\Delta T_*$ for the enclosure). The mean variables and their corresponding fluctuating quantities have the scaling variables and so non-dimensionalization is based on the following set of general scaling variable;

$$\left.\begin{array}{llll} X_j = X_j' & U_j = U_j' U_* & P = P' P_o & \Theta = \dfrac{T - T_*}{\Delta T_*} \\ K = K' U_* & \varepsilon = \varepsilon' \dfrac{U_*^3}{L_o} & t = t' \dfrac{L_o}{U_*} & \mu = \mu' \mu_0 \\ \mu_s = \mu_s' \mu_0 & V = V' \mu_0 \rho = \rho' \rho_0 = C_R C_{PP} & \lambda = \lambda' \lambda_0 & \end{array}\right\} \quad (3.78)$$

In which L_0 is the characterized length, ΔT_* is the characterized temperature difference and T_* is a convenient temperature that will result in Θ being bounded in the solution region. The prime denotes a no-dimensional quantities and the subscript $*$ denotes a variable that can be arbitrarily defined to specify a non-dimensional scheme. The main rationale behind non-dimensionalisation is to reduce the number of parameters, (Jiyuan *et al.*, 2012). To apply these variables in the continuity equation (3.72) gives the following equation;

$$\frac{\partial \rho}{\partial t} = \frac{\partial \rho}{\partial \rho'} \frac{\partial \rho'}{\partial t'} \frac{\partial t'}{\partial t} = \frac{P_0 U_*}{L_0} \frac{\partial \rho'}{\partial t'}$$

$$\frac{\partial U_j}{\partial x_j} = \frac{\partial U_j}{\partial U_j'} \frac{\partial U_j'}{\partial x_j'} \frac{\partial x_j'}{\partial x_j} = \frac{U_* \partial U_j'}{L_0 \partial x_j'}$$

$$\rho \frac{\partial U_j}{\partial x_j} = \frac{U_{*\rho' \rho_0}}{L_0} \frac{\partial U_j'}{\partial x_j'}$$

$$\frac{\partial \rho}{\partial x_j} = \frac{\partial \rho}{\partial \rho'} \frac{\partial \rho'}{\partial x_j'} \frac{\partial x_j'}{\partial x_j} = \frac{\rho_0}{L_0} \frac{\partial \rho'}{\partial x_j'}$$

$$U_j \frac{\partial \rho}{\partial x_j} = \frac{\rho_0 U_j' U_*}{L_0} \frac{\partial \rho'}{\partial x_j'}$$

But;

$$\frac{\partial(\rho U_j)}{\partial x_j} = \rho \frac{\partial U_j}{\partial x_j} + U_j \frac{\partial \rho}{\partial x_j}$$

Therefore;

$$\frac{\partial(\rho U_j)}{\partial x_j} = \frac{U_{*\rho'\rho_0}}{L_0} \frac{\partial U_j{}'}{\partial x_j{}'} + \frac{\rho_0 U_j{}' U_*}{L_0} \frac{\partial \rho'}{\partial x_j{}'} = \frac{\rho_0 U_*}{L_0} \left(\rho' \frac{\partial U_j{}'}{\partial x'_j} + U'_j \frac{\partial \rho'}{\partial x'_j} \right) = \frac{\rho_0 U_*}{L_0} \frac{\partial(\rho' U'_j)}{\partial x'_j}$$

Similarly;

$$\frac{\partial \overline{(\rho U_j)}}{\partial x_j} = \overline{\frac{\partial(\rho U_j)}{\partial x_j}}$$

But;

$$\frac{\partial(\rho U_j)}{\partial x_j} = \frac{\rho_0 U_*}{L_0} \frac{\partial(\rho' u'_j)}{\partial x'_j}$$

Therefore;

$$\frac{\partial \overline{(\rho U_j)}}{\partial x_j} = \frac{\rho_0 U_*}{L_0} \frac{\partial \overline{(\rho' u'_j)}}{\partial x'_j}$$

Adding all the non-dimensional form for continuity equation yields;

$$\frac{P_0 U_*}{L_0} \frac{\partial \rho'}{\partial t'} + \frac{\rho_0 U_*}{L_0} \frac{\partial(\rho' U'_j)}{\partial x'_j} + \frac{\rho_0 U_*}{L_0} \frac{\partial \overline{(\rho' u'_j)}}{\partial x'_j} = 0$$

This simplifies to;

$$\frac{P_0 U_*}{L_0} \frac{\partial \rho'}{\partial t'} + \frac{\rho_0 U_*}{L_0} \frac{\partial}{\partial x_j} \left(\rho' U'_j + \overline{\rho' u'_j} \right) = 0$$

Diving through by $\frac{P_0 U_*}{L_0}$ yields;

$$\frac{\partial \rho'}{\partial t'} + \frac{\partial}{\partial x_j}\left(\rho' U'_j + \overline{\rho' u'_j}\right) = 0 \tag{3.78}$$

The same procedure is applied to the mean momentum equation (3.73), the mean energy equation (3.74), the turbulent kinetic equation (3.76) and the specific dissipation equation (3.77) yielding the following equations respectively;

$$\frac{\partial}{\partial t}\left(\rho U'_j + \overline{\rho u'_i}\right) + \frac{\partial}{\partial x_j}\left(\rho U'_i U'_j + U'_i\overline{\rho' u'_j}\right) = -\left\{\frac{P_0}{P_0 U_*^2}\right\}\frac{\partial P'}{\partial x'_i} + \left\{\frac{gL_0}{U_*^2}\right\}\rho g'_i + \frac{\partial}{\partial x_j}\left(\left\{\frac{\mu_0}{P_0 U_* L_0}\right\}\tau_{ij} - U'_j\overline{\rho' u'_j} - \rho'\overline{u'_i u'_j} - \overline{\rho' u'_i u'_j}\right) \tag{3.79}$$

$$\frac{\partial}{\partial t'}\left(c'_P\rho'\Theta + c'_P\overline{\rho'\theta}\right) + \frac{\partial}{\partial x'_j}\left(c_P\overline{\rho' U'_j\Theta}\right) = \left\{\frac{P_0}{c_{P0}\rho_0\Delta T_*}\right\}\left[\frac{\partial P'}{\partial t'} + U'_j\frac{\partial P'}{\partial x'_j} + u'_j\frac{\partial p'}{\partial x_j}\right] + \frac{\partial}{\partial x'_j}\left(\left\{\frac{\lambda_0}{c_{P0}\rho_0 U_* L_0}\right\}\lambda\frac{\partial\Theta}{\partial x'_j} - c_P\overline{\rho' U'_j\theta} - c_P\overline{\rho' U'_j\theta}\right) + \left\{\frac{\mu_0 U_*}{c_{P0}\rho_0\Delta T_* L_0}\right\}\emptyset \tag{3.80}$$

$$\frac{\partial}{\partial t'}\rho' k' + \frac{\partial}{\partial x_j}\rho' U'_j k' = \left\{\frac{\mu_0}{\rho_0 U_* L_0}\right\}\overline{u'_j\frac{\partial}{\partial x'_j}u'_j\left(\frac{\partial u'_i}{\partial x'_j} + \frac{\partial u'_j}{\partial x'_j}\right)} - \rho'\overline{u'_i u'_j}\frac{\partial U'_i}{\partial x'_j} - \frac{1}{2}\frac{\partial}{\partial x_j}\overline{\rho' u'_i u'_j} + \left\{\frac{gL_0}{U_*^2}\right\}p' U'_i - \left\{\frac{P_0}{P_0 U_*^2}\right\}\overline{u'_j\frac{\partial P'}{\partial x'_j}} \tag{3.81}$$

$$\frac{\partial}{\partial t'}\rho'\omega' + \frac{\partial}{\partial x_j}P' U'_j\omega' = -\left\{\frac{\mu_0}{\rho_0 U_* L_0}\right\}\frac{\partial}{\partial x'_k}\left(\overline{\mu'\mu'_k\frac{\partial u'_i}{\partial x'_j}\frac{\partial\mu'_j}{\partial x'_j}} + 2\left\{\frac{P_0}{P_0 U_*^2}\right\}\nu'\overline{\frac{\partial\mu'_k}{\partial x'_l}\frac{\partial P'}{\partial x'_l}} - \mu'\frac{\partial\varepsilon'}{\partial x'_k}\right) - 2\left\{\frac{\mu_0}{\rho_0 U_* L_0}\right\}\mu'\overline{\frac{\partial u'_j}{\partial x'_k}\frac{\partial u'_i}{\partial x'_j}\frac{\partial u_k}{\partial x'_j}} - 2\left\{\frac{\mu_0^2}{P_0^2 U_*^2 L_0^2}\right\}\overline{P}'\left(\nu'\frac{\partial^2 u_i}{\partial x'_k\partial x'_j}\right) + 2\left\{\frac{\mu_0}{\rho_0 U_* L_0}\right\}\mu'\frac{\partial u'_j}{\partial x'_k}\left(\overline{\frac{\partial u'_i}{\partial x'_j}\frac{\partial u'_k}{\partial x'_j}} + \frac{\partial u'_i}{\partial x'_j}\overline{\frac{\partial u'_j}{\partial x'_i}}\right) - 2\left\{\frac{\mu_0}{\rho_0 U_* L_0}\right\}\mu'\frac{\partial^2 u_i}{\partial x'_k\partial x'_j}\overline{\mu'_k\frac{\partial u}{\partial x'_j}} \tag{3.82}$$

From this point, all equation and variables referred will be non-dimensional. To avoid ambiguity, the primes that indicate non-dimensionality have been avoided for the remainder of this work.

Using a non-dimensional scheme presented above, equations (3.78), (3.79), (3.80), (3.81) and (3.82) in general from becomes

$$\frac{\partial \rho}{\partial t} + \frac{\partial}{\partial x_j}\left(\rho U_i + \overline{\rho u_j}\right) \tag{3.83}$$

$$\frac{\partial}{\partial t}\left(\rho U_i + \overline{\rho u_j}\right) + \frac{\partial}{\partial x_j}\left(\rho U_i U_j + U_i\overline{\rho u_j}\right) = -N_1\frac{\partial P}{\partial x_i} + N_2 p g_i + \frac{\partial}{\partial x_j}\left(N_3\tau_{ij} - U_i\overline{\rho u_\iota} - \overline{\rho u_\iota u_J} - \rho\overline{u_\iota u_j}\right) = 0 \tag{3.84}$$

$$\frac{\partial}{\partial t}\left(c_P\rho\Theta + c_P\overline{\rho\Theta}\right) + \frac{\partial}{\partial x_j}\left(c_P\overline{\rho U_J\Theta}\right) = L_1\left[\frac{\partial \rho}{\partial t} + U_j\frac{\partial p}{\partial x_j} + \overline{u_J\frac{\partial p}{\partial x_J}}\right] + \frac{\partial}{\partial x_j}\left(L_2\lambda\frac{\partial\Theta}{\partial x_j} - c_P\overline{\rho\Theta} + c_P\rho\Theta\right) + L_3\emptyset \tag{3.85}$$

$$\frac{\partial}{\partial t}\rho k + \frac{\partial}{\partial x_j}(\rho U_i k) = A_1\overline{u_J\frac{\partial \mu}{\partial x_J}}\left(\frac{\partial u_i}{\partial x_j} + \frac{\partial u_j}{\partial x_i}\right) - \frac{1}{2}\frac{\partial}{\partial x_j}\overline{\rho u_\iota u_J}\frac{\partial U_i}{\partial U_j} + B_2\overline{\rho u_\iota}g_i - B_3\overline{u_J\frac{\partial p}{\partial x_\iota}} \tag{3.86}$$

$$\frac{\partial}{\partial t}\rho\omega + \frac{\partial}{\partial x_j}(\rho U_i\omega) = -\frac{\partial}{\partial x_k}\left(B_1\overline{\mu u_k\frac{\partial u_\iota}{\partial x_J}\frac{\partial u_\iota}{\partial x_J}} + 2B_2\nu\frac{\partial u_k}{\partial x_i}\frac{\partial u_\rho}{\partial x_i} - B_1\mu\frac{\partial\omega}{\partial x_k}\right) - 2B_1\mu\frac{\partial U_i}{\partial x_j}\left(\frac{\partial u_i}{\partial x_j}\frac{\partial u_k}{\partial x_j} + \frac{\partial u_j}{\partial x_j}\frac{\partial u_i}{\partial x_k}\right) - 2B_1\mu\frac{\partial^2 U_i}{\partial x_j\partial x_k}\overline{\mu_k\frac{\partial u_\iota}{\partial x_J}} \tag{3.87}$$

Where the coefficients;

N_1 , $N_2, N_3, L_1, L_2, L_3, A_1, A_2, A_3, B_1, B_2, B_3,$ and B_4 are indicated in table 3.1 below.

Symbol	Coefficient	Scheme
U_*		$\sqrt{g\beta\Delta T L_0}$
N_1	$-\frac{P_0}{P_0 U_*^2}$	$\frac{EU_*F_0}{\zeta\eta}$
N_2	$\frac{gL_0}{U_*^2}$	$\frac{1}{\zeta\eta}$

N_3	$\frac{\mu_0}{P_0 U_* L_0}$	$\frac{1}{\sqrt{G_0}}$
L_1	$\frac{P_0}{c_{P0}\rho_0 \Delta T_*}$	$E_\mu E_C$
L_2	$\frac{\lambda_0}{c_{P0}\rho_0 U_* L_0}$	$\frac{1}{P_r\sqrt{G_0}}$
L_3	$\frac{\mu_0 U_*}{c_{P0}\rho_0 \Delta T_* L_0}$	$E_\mu R_e^{-1}$
A_1	$\frac{\mu_0}{\rho_0 U_* L_0}$	$\frac{1}{\sqrt{G_0}}$
A_2	$\frac{gL_0}{U_*^2}$	$\frac{1}{\zeta\eta}$
A_3	$\frac{p_0}{\rho_0 U_*^2}$	$\frac{E_\mu F_0}{\zeta\eta}$
B_1	$\frac{\mu_0}{\rho_0 U_* L_0}$	$\frac{1}{\sqrt{G_0}}$
B_2	$\frac{\mu_0 P_0}{U_*^2 L_0 U_*^2}$	$\frac{E_\mu}{\sqrt{G_0}}$
B_3	$\left(\frac{\mu_0}{P_0 U_* L_0}\right)^2$	$\frac{1}{\sqrt{G_0}}$
B_4	$\frac{g\mu_0}{P_0 U_*^3}$	$\frac{F_0}{\sqrt{G_0}}$

Table 3.1 Coefficient for Non-dimensional Governing Equations (3.84) – (3.87)

The non-dimensionalized problem will now only have three parameters (Re, Ra, and Pr) due to the aggregation of the non-dimensional parameters.

3.6 Model Description

In this project, a numerical investigation of turbulent natural convection flow within a 2-D is conducted. The geometry is illustrated in figure 3.3. It consists of a hot surface, located on the left side of the square cavity wall, and a cold surface on the right side. The enclosure is heated on the hot wall (Red color) and cooled on the cold wall (blue color).The walls measure 1m by 1m. The hot and cold walls were maintained at 313K and 293K respectively. Each of the remaining walls were adiabatic. The Rayleigh number was varied from 10^9 to 10^{11}.

All boundaries of the enclosure are stationary, non-slip, rigid and impermeable. The fluid to be used is air. Aspect ratio A=H/L=1, where H is the height and L is the length of the enclosure. The characteristic length is taken to be the size of the enclosure in the x – direction.

Initially, air is motionless the temperature of which is equal to the average temperature of the vertical walls. The temperature of the hot wall and that of the cold wall were varied such that $T_h > T_c$ where T_h is the temperature of the hot wall and T_c the temperature of the cold wall. This implies that the density gradient of the internal air is normal to the gravity and the buoyancy- driven natural convection starts immediately the heat is applied. Due to the buoyancy, a fluid motion is induced in the enclosure depending on the enclosure geometry (i.e. aspect ratio A=H/L), the working fluid (which in this study is air) and temperature difference $\Delta T = T_h - T_c$.

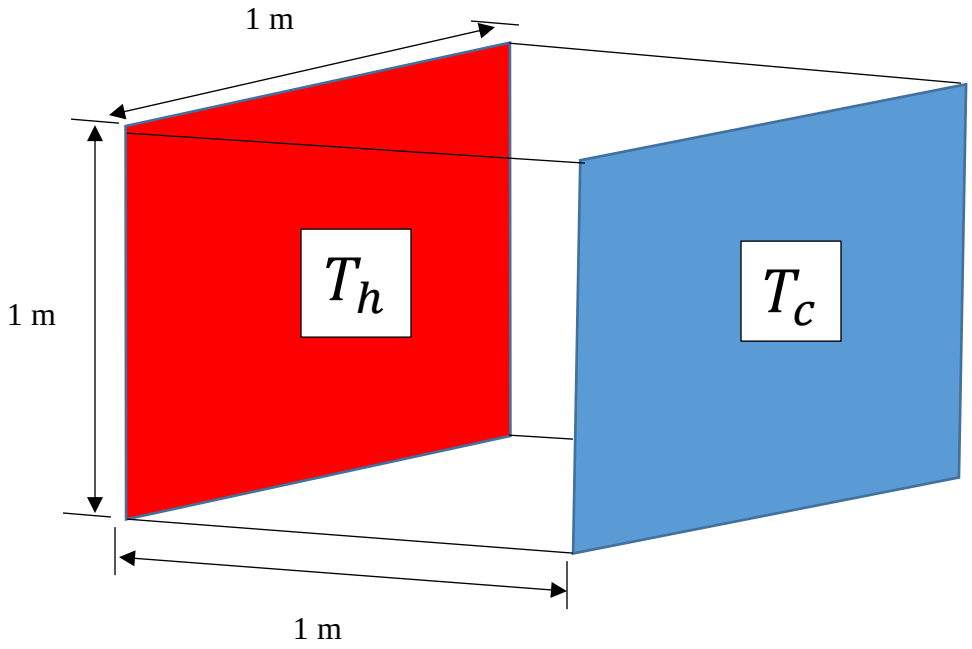

Fig. 3.3 Geometry of the 3-d numerical model

We use the PISO algorithm and the finite Volume Method to numerically investigate the velocity, temperature and pressure profile of air in this 2-d enclosure, any change in terms of accuracy and convergence time and any additional profile.

3.7 Boussinesq Approximation

The Boussinesq approximation is used if the mach number of the flow is small, no sound or shock wave propagation is considered, the vertical scale of flow is not too great, and temperature differences in the fluid are small (Boussinesq 1903). The following Boussinesq assumptions are made. Except for the density in the buoyancy, all physical properties of the fluid are constant.

i. All physical properties of the fluid are constant except the density in the buoyancy

ii. The fluid is Newtonian (i.e. exhibits a linear relationship between the shear stress and the velocity gradient) and that there is no internal heat source

iii. The variation of density is small hence negligible, however even weak density variations are important in Buoyancy and so we shall retain variation in density due to buoyancy forces in the vertical equation of motion. We define buoyancy as;

$$b = g\frac{(\rho - \rho_0)}{\rho_0}$$

Where $(\rho - \rho_0)$ is the density variation due to buoyancy force ρ_0 the constant fluid density and g the gravitational force.

i) The variation of density ρ due to buoyancy forces is propotional to the temperature difference ΔT.

ii) The viscous dissipation effect may be neglected

Since the density in the buoyancy term varies only with temperature and this variation is small, it follows that;

$$\rho = \rho_0 + (T - T_0)(\frac{\partial \rho}{\partial T})T_0 \quad (3.89)$$

The coefficient of the expansion at constant pressure is defined as

$$\beta_0 = \frac{1}{\rho_0}(\frac{\partial \rho}{\partial T})T_0 \quad (3.90)$$

Re-arranging Eq. (3.90) yields;

$$\rho_0\beta_0 = (\frac{\partial \rho}{\partial T})T_0 \quad (3.91)$$

Substitution of Eq. (3.91) into (3.89)

$$\rho = \rho_0 + \rho_0\beta_0(T - T_0) \tag{3.92}$$

Further re-arrangement of Eq. (3.92) using equation (3.91)

$$\rho = \rho_0[1 + \beta_0(T - T_0)] \tag{3.93}$$

3.8 Simplifying Governing Equations

Using the Boussinesq approximation and making use of the figure (3.93) into the governing equations, the equation governing natural convention of air in the enclosure are presented in non-dimensional for an incompressible turbulent flow as follows:

The continuity equation (3.83) becomes

$$\frac{\partial U_j}{\partial x_j} = 0 \tag{3.94}$$

The momentum equation (3.84) becomes

$$\frac{\partial \rho U_j}{\partial t} + \frac{\partial}{\partial x_j}\rho U_i U_j = -\frac{\partial P}{\partial x_j} + \rho_0[1 + \beta_0(T - T_0)]g_i + \frac{\partial}{\partial x_j}\left[\mu\left(\frac{\partial U_i}{\partial x_j} + \frac{\partial U_i}{\partial x_i}\right) - \overline{u_\iota u_\jmath}\right] \tag{3.95}$$

The energy equation (3.85) becomes;

$$\frac{\partial T}{\partial t} + \frac{\partial}{\partial x_j}U_j T = \frac{\partial}{\partial x_j}\left(\frac{\lambda_0}{c_{P0}\rho_0 U_* L_0}\frac{\partial T}{\partial x_j} - \overline{u_\jmath T}\right) \tag{3.96}$$

The turbulent kinetic energy equation (3.86) simplifies to

$$\frac{\partial T}{\partial t} + \frac{\partial}{\partial x_j}U_j k = \frac{\mu_0}{P_0 U_* L_0}\overline{u_\jmath \frac{\partial}{\partial x_\jmath} v\left(\frac{\partial u_\iota}{\partial x_\jmath} + \frac{\partial u_\jmath}{\partial x_\iota}\right)} - \frac{\partial}{\partial x_j}\overline{u_\jmath\left(\frac{u_\iota u_\iota}{2} + \frac{P}{\rho}\right)} - \overline{u_\iota u_\jmath}\frac{\partial U_j}{\partial x_j} + \frac{gL_0}{U_*^2}\frac{\overline{\rho u_\jmath} g_i}{\rho} \tag{3.97}$$

Or

$$\frac{\partial k}{\partial t} + \frac{\partial}{\partial x_j} U_j k = \overline{u_j \frac{\partial}{\partial x_j} v \left(\frac{\partial u_\iota}{\partial x_j} + \frac{\partial u_j}{\partial x_\iota} \right)} - \frac{\partial}{\partial x_j} \overline{u_j \left(\frac{u_\iota u_\iota}{2} + \frac{P}{\rho} \right)} + P_k + G_k \quad (3.98)$$

Where:

$$P_k = \overline{u_\iota u_j} \frac{\partial U_j}{\partial x_j}, \text{ and } G_k = \frac{\overline{\rho u_j} g_i}{\rho} \quad (3.99)$$

Specific dissipation equation (3.87) becomes;

$$\frac{\partial}{\partial t}(\rho\omega) + \frac{\partial}{\partial x_i}(\rho\omega u_i) = \frac{\partial}{\partial x_j}\left[\left(\mu + \frac{\mu_t}{\sigma_\omega}\right)\frac{\partial \omega}{\partial x_j}\right] + G_\omega - Y_\omega + D_\omega \quad (3.100)$$

Where $\widetilde{G_\omega}$ represents the generation of turbulent kinetic energy that arises due to mean velocity gradient and G_ω is the generation of ω which are defined in the exact manor as the K - epsilon model. Y_k and Y_ω represent the dimension of κ and ω due to turbulence. α_K and α_ω are turbulent Prantl numbers for k and ω respectively. Although the density variations are neglected everywhere in our case we note that where they cause buoyancy forces, like in the G_k term of equation (3.99) they are not neglected. These terms contribute to the generation of motion and thus cannot be neglected (Gatheri, 1994).

$$\sigma_{\omega,1} = 2.0,\ \sigma_{\omega,2} = 1.168\ ,\ \sigma_{k,1} = 1.176,\ \sigma_{k,2} = 1.0\ ,\ a_1 = 0.31,\ \beta_{i,2} = 0.0828,$$
$$\beta_{i,1} 0.075 \quad (3.101)$$

The transport equation for the SST $\kappa - \omega$ model can also be written in terms of effective diffusivity of κ andω, as;

$$\frac{\partial}{\partial t}(\rho\kappa) + \frac{\partial}{\partial x_i}(\rho\kappa u_i) = \frac{\partial}{\partial x_j}\left[\Gamma_\kappa \frac{\partial k}{\partial x_j}\right] + \widetilde{G_\omega} - Y_k + Y_k \quad (3.102)$$

$$\frac{\partial}{\partial t}(\rho\omega) + \frac{\partial}{\partial x_i}(\rho\omega u_i) = \frac{\partial}{\partial x_j}\left[\Gamma_\omega \frac{\partial \omega}{\partial x_j}\right] + G_\omega - Y_\omega + D_\omega + S_\omega \quad (3.103)$$

Where Γ_κ and Γ_ω represent the effective diffusivity of κ and ω, respectively, which are given as;

$$\left.\begin{aligned}\Gamma_\kappa &= \mu + \frac{\mu_t}{\sigma_\omega}\\ \Gamma_\omega &= \mu + \frac{\mu_t}{\sigma_\omega}\end{aligned}\right\} \quad (3.104)$$

3.9.1 Dissipation of κ

The term Y_κ represent the dissipation of turbulence kinetic energy, and is defined in a similar manner as in the standard $\kappa - \omega$ model. The difference is as follows:

- In the standard $\kappa - \omega$ model, f_{β^*} is defined as a piecewise function. For the SST $\kappa - \omega$ Model, f_{β^*} is a constant equal to 1. Thus;

$$Y_\kappa = \rho\beta^*\kappa\omega$$

3.9.2 Dissipation of ω

The term Y_ω represents the dissipation of ω and is defined in a similar way as in the standard model $\kappa - \omega$ model. The difference is as follows;

- In the standard $\kappa - \omega$ model, $\beta_i = 0.072$ and f_β is defined in the equation (3.105) as;

$$\left.\begin{aligned} f_\beta &= \frac{1+70x_\omega}{1+80x_\omega}\\ x_\omega &= \left|\frac{\Omega_{ij}\Omega_{ij}\Omega_{ij}}{(\beta^*_\infty)^3}\right|\\ \Omega_{ij} &= \frac{1}{2}\left(\frac{\partial u_i}{\partial x_j} - \frac{\partial u_j}{\partial x_i}\right)\end{aligned}\right\} \quad (3.105)$$

For the SST $\kappa - \omega$ model, f_β is a constant equal to 1. Thus, $Y_\omega = \rho\beta^*\omega^2$ becomes

$$Y_\omega = \rho\beta f_{\beta^*}\kappa\omega^2 \tag{3.106}$$

Instead of having a constant value, β_i is given by;

$$\beta_i = F_1\beta_{i,1} + (1 - F_1)\beta_{i,2} \tag{3.107}$$

3.10 Boundary conditions

The following boundary conditions will apply for PISO algorithms.

3.10.1 Temperature Boundary conditions

The choice of the non-dimensional Θ temperature will be such that$0 \leq \Theta \leq 1$; where $\Theta = (T - T_*)/\Delta T_*$ so Θ is set at 1 on the hot wall and Θ is zero at the cold wall. ΔT_* is the characteristics temperature difference between the hot and cold surfaces, i.e $\Delta T_* = T_h - T_c$ in which T_h is the temperature of the hot wall and T_c is the temperature of the cold wall.

3.10.2 Thermal Boundary conditions

The problem at hand involves heating the left part of one wall and cooling on the right part of the same wall, the two thermal conditions that were used are

- Isothermal – for the vertical walls, represented by the equation Θ = Constant. On the hot wall and the cold wall , the Dirchlet boundary condition apply in which $\Theta_{hot} = 1$ and $\Theta_{cold} = 0$.
- Adiabatic –The temperature of the remaining upper and lower walls were kept constant
-

3.10.3 Velocity Boundary conditions

No slip boundary condition is used. This implies at the solid boundary, the viscous fluid will have zero velocity relative to the wall this is because, the particles of air close to the surface will not

move along with the flow, given that the adhesive force is greater than the cohesive force consequently, the outermost molecule of the fluid are stuck to the surface upon which it flows. Hence $u = v = w = 0$ at the surface

Free slip boundary condition is used. In this square enclosure, each boundary is assumed impermeable. This implies the component of velocity normal to the surface/boundary is zero justifiably mass cannot penetrate an impermeable solid surface.

3.10.4 Pressure Boundary conditions for the Pressure-Correction Equation

Let the guessed pressure field $p^* = 760mmHg$. Then the value of p'at the boundary will be zero. It is useful to start from $p' = 0$ as the guess for all points, so that the solution for p' does not acquire a large absolute value.

CHAPTER FOUR

THE NUMERICAL METHOD

4.1 Introduction

After the conservation laws governing heat transfer, fluid flow and other related processes are expressed in differential form and modeled inform of temperature and velocity, they can be solved using numerical methods, rather than analytical methods, determine pressure, temperature and mass flux for various boundary conditions.

A discretized equation is an algebraic relationship that connects the values of the dependent variable to a group of grid points within a control volume. Due to computational limitations, the number of locations is finite.

Our method for deriving the discretization is control volume formulation. To ensure that the discretization equation results are not dependent on the profile assumptions, the solution is checked for mesh independence. In the iterative process for solving a discretization equation, it is desirable to use over-relaxation and under-relaxation factors in order to speed up and slow down the changes, from iteration to iteration, in the values of the dependent variable. This is to avoid divergence rather improve convergence ability.

4.2 Discretization of the Solution Domain

The procedure of dividing the computing domain into a finite number of contagious control volumes, and the statements that result expressing the exact conservation of associated properties for each control volume, is known as space discretization. Variable values are calculated at the centroid of each control volume, variable values at the control volume surface are expressed in terms of center values using interpolation, and surface and volume integrals are approximated using suitable quadrature formulae..

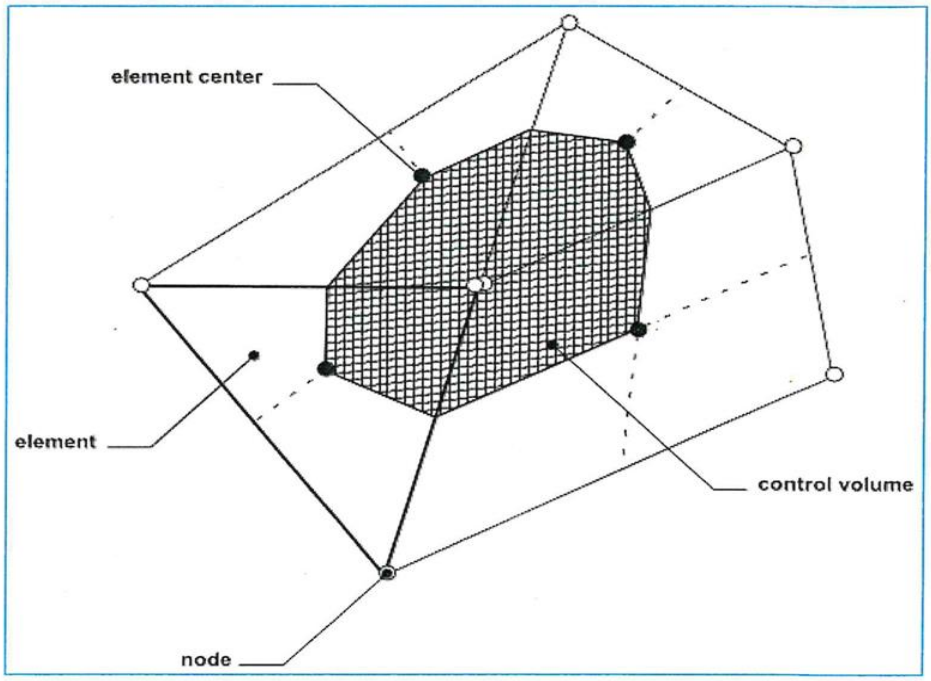

Fig. 4.1 Control-volume element

Fig. 4.1 Control-volume element.

4.3 Discretization of the Continuity Equation by FVM

Consider the continuity equation (3.94) integrating the equation and applying Gauss' divergence theorem to the volume integral, we get:

$$\frac{1}{\Delta V}\int_v \bar{V}.UdV = \frac{1}{\Delta V}\int_A UdA \tag{4.1}$$

Assuming that the velocity variable on the face is represented by its centroid value, we may write:

$$\frac{1}{\Delta V}\int_A UdA = \frac{1}{\Delta V}\sum_i U_i A_i \tag{4.2}$$

For a derivative of first order of U in two dimensions, the term along the x direction represented in equation (3.94), can be written as;

$$\left(\frac{\partial u}{\partial x}\right) = \frac{1}{\Delta V}\int_V \frac{\partial u}{\partial x} dV = \frac{1}{\Delta V}\int_A \; u dA^x \approx \frac{1}{\Delta V}\sum_{i=1}^{N} u_i A_i^x \tag{4.3}$$

Where N is the number of bounding surfaces on the elemental volume and u_i is the velocity variable. In the same way, a first-order derivative of *U* in the *y* direction can be calculated and written as;

$$\left(\frac{\partial v}{\partial y}\right) = \frac{1}{\Delta V}\int_{\Delta V} \frac{\partial v}{\partial y} dV = \frac{1}{\Delta V}\int_A \; u dA^y \approx \frac{1}{\Delta V}\sum_{i=1}^{N} v_i A_i^y \tag{4.4}$$

It follows from equation (4.2) the derivative of first order of *U* in the z direction can be written as;

$$\left(\frac{\partial w}{\partial y}\right) = \frac{1}{\Delta V}\int_{\Delta V} \frac{\partial w}{\partial y} dV = \frac{1}{\Delta V}\int_A \; W dA^z \approx \frac{1}{\Delta V}\sum_{i=1}^{N} W_i A_i^z \tag{4.5}$$

For our considered mesh (orthogonal) in figure 4.2, using equations (4.2), (4.3) and (4.4), we get:

$$(u_e - u_w)\Delta y + (v_n - v_s)\Delta x = 0 \tag{4.6}$$

In 3-D, equation (4.6) becomes;

$$[(\rho u)_e - (\rho u)_w]\Delta y \Delta z + [(\rho v)_n - (\rho v)_s]\Delta z \Delta x + [(\rho w)_t - (\rho w)_b]\Delta x \Delta y = 0 \tag{4.7}$$

4.5 Discretization of the Momentum Equation by FVM

Consider the 2-D rectangular domain shown in figure 4.2. Assume that;

i. The velocity vector U and the pressure P are stored at the cell centroids.

ii. A steady state.

The momentum equation in equation (3.95) in x and y may be written as;

$$\nabla.(\rho V u) = \nabla.(\mu \nabla u) - \nabla P.i + S_u \tag{4.8}$$

$$\nabla.(\rho V v) = \nabla.(\mu \nabla u) - \nabla P.i + S_v \tag{4.9}$$

Each of the momentum equations contains a pressure gradient term, a source term ($S_u \; and \; S_v$) which contains the force term as well as the stress tensor term's remnants

Let's look at the x-direction pressure gradient definition. We combine the governing equations (4.8) over the cell volume to derive discrete equations. To integrate the pressure gradient over the control volume, we apply the gradient theorem, which yields;

$$\int_A \; \nabla P d\vartheta = \int_A \; P dA = \left(P_e - P_p\right) A_e \tag{4.10}$$

Assume that pressure at the face centroid represents the mean value on the face, $P_P - P_E$ represents the pressure difference, and A_e represents the pressure difference's acting region. For the diffusion terms expressed in the momentum equation (4.8), a second order derivative along the *x* direction can be calculated as follows: Consider the generic variable's ∅steady-state diffusion in a one-dimensional domain. The equation that governs such a process is given by;

$$\frac{\partial}{\partial x}\left(\Gamma \frac{\partial \emptyset}{\partial x}\right) + S_\emptyset = 0 \tag{4.11}$$

Where $S_\emptyset$ is the source sentence and Γ is the diffusion coefficient. Equation (4.11) can be approximated by using equation to apply finite-volume discretization to the gradient term (4.3).

This gives;

$$\frac{\partial}{\partial x}\left(\Gamma \frac{\partial u}{\partial x}\right) + S_u$$

$$= \frac{1}{\Delta V}\int_V \left[\frac{\partial}{\partial x}\left(\Gamma\frac{\partial u}{\partial x}\right) + S_u\right] dV$$

$$= \frac{1}{\Delta V}\int_A \left(\Gamma\frac{\partial u}{\partial x}\right) dA^x + \frac{1}{\Delta V}\int_{\Delta V} S_u dV \approx \frac{1}{\Delta V}\sum_{i=1}^{2}\left(\Gamma\frac{\partial u}{\partial x}\right)_i A_i^z + \frac{1}{\Delta V}\int_{\Delta V} S_u dV \qquad (4.12)$$

Where, A$A_1^x = -A_W$ and $A_2^x = -A_E$, are used to represent the projected regions A_i^x in the one-dimensional case, and the source term S_u is believed to be constant within ΔV,, which is the finite-control volume. The discretized equation's final form is as follows:

$$\frac{1}{\Delta V}\left(\Gamma\frac{\partial u}{\partial x}\right)_e A_E - \frac{1}{\Delta V}\left(\Gamma\frac{\partial u}{\partial x}\right)_w A_w + S_u = 0 \qquad (4.13)$$

Expressing equation (4.13) in algebraic form becomes;

$$\frac{\Gamma_e A_E}{\Delta V}\left(\frac{u_e - u_p}{\delta x_E}\right) - \frac{\Gamma_w A_W}{\Delta V}\left(\frac{u_p - u_w}{\delta x_W}\right) + S_u = 0 \qquad (4.14)$$

Equation (4.14) is the discretized equation and possesses a clear physical interpretation. It can be rearranged as;

$$\frac{1}{\Delta V}\left(\frac{\Gamma_e A_E}{\delta x_E} + \frac{\Gamma_w A_w}{\delta x_w}\right) u_p = \frac{1}{\Delta V}\left(\frac{\Gamma_e A_E}{\delta x_E}\right) u_E + \frac{1}{\Delta V}\left(\frac{\Gamma_w A_w}{\delta x_w}\right) u_w + S_u \qquad (4.15)$$

As above, by identifying the coefficients of u_E and u_w in equation (4.15) as a_E and a_W and the coefficient of u_p as $a_{p,}$ the algebraic form can be written as;

$$a_p u_p = a_E u_E + a_w u_w + b \qquad (4.16)$$

Where;

$a_E = \frac{\Gamma_e A_E}{\Delta V \delta x_E}$ $\quad a_w = \frac{\Gamma_w A_w}{\Delta V \delta x_w}$ $\quad a_p = a_E + a_w$ and $b = S_u$

The discretized form for equation (4.16) is represented by the finite-volume approach (4.11). Because Δy and Δz have unit length dimensions, the face regions A_E and A_w are unity for the one-dimensional problem considered here; the finite-control volume ΔV is therefore the width Δx.

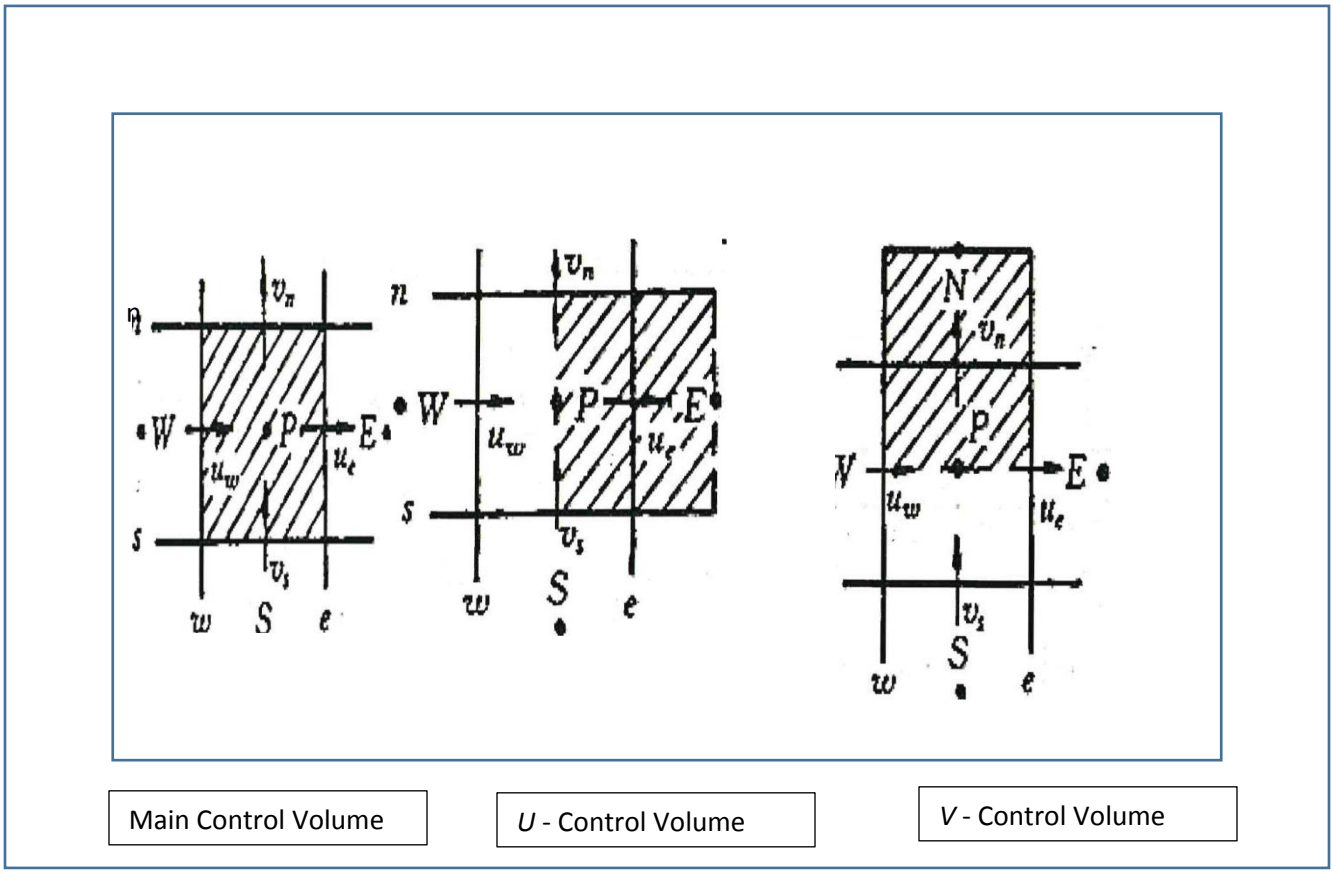

Fig 4.2 The Staggered Grid $\frac{\partial p}{\partial x} = \frac{P_E - P_P}{(\partial x)_e} \frac{\partial p}{\partial x} = \frac{P_N - P_P}{(\partial y)_n}$

Let $a_E u_E + a_w u_w = a_{nb} u_{nb}$, using equations (4.8), (4.10) and (4.16), and a displaced or staggered grid for the velocity components as in figure 4.3, as used by Harlow and Welch (1965) in their MAC method, the resulting discretized momentum equation, in x-direction, can be written

$$a_e u_e = \sum a_{nb} u_{nb} + b + (P_P - P_E) A_e \qquad (4.17)$$

The number of neighbor terms will be determined by the problem's dimensionality. Six neighbor $u's$ would be included in this three-dimensional case, where a_e is the primary grid point coefficient and a_{nb} are the neighbor coefficients that account for the combined convection-diffusion at the control-volume faces. The principal grid point is denoted by the letter *P*. Its faces are located between the point e and the sites of the neighboring $u's$. The faces regular to that direction pass through the major grid points P and E, so the staggering is only in the x direction.

Advantage – the difference $P_P - P_E$ can be used to calculate the pressure force acting on the control volume for the velocity u; $b = S_c \Delta x \Delta y + a_P^o \emptyset_P^o$ in which S_c is the source term quantity; $a_P^o = \frac{\rho_P^o \Delta x \Delta y \Delta z}{\Delta t}$, $\emptyset_P^o$ is known value of the unsteady term at the time *t* i.e., at the beginning of the time step. The pressure term gives rise to the last term in equation (4.13). Since the pressure field will also be ultimately calculated, it is convenient to bury the pressures in the source term. The term $(P_P - P_E)A_e$ is the pressure force acting on the *u* control volume, A_e being the area which the pressure difference acts. For three-dimensional case, A_e will stand for $\Delta y \Delta z$.

In a similar way, the momentum equations for the other directions are dealt. The y-direction momentum equation, for example, is staggered in the y-direction. Hence the discretization equation for v_n is given as;

$$a_n v_n = \sum a_{nb} v_{nb} + b + (P_P - P_N) A_n \tag{4.18}$$

Where $(P_P - P_N)A_n$ is the pressure force acting on the *v* control volume, where A_n is the area which the pressure difference acts. (For 3-D case, A_n stands for $\Delta x \Delta z$.) Similarly, the *z*-direction momentum equation is staggered in the *z* – direction and given as;

$$a_n w_t = \sum a_{nb} w_{nb} + b + (P_P - P_t) A_t \tag{4.19}$$

Where $(P_P - P_N)A_n$ is the appropriate pressure force. Where the location *t*, lies on the *z* – direction grid line between grid points *P* and *T*, Pantakar *et al* (1980), where; $(P_P - P_t)A_t$ is the pressure force acting on the *w* control volume, where A_n is the area which the pressure difference acts. (For 3 – D case, A_t stands for $\Delta x \Delta y$). Only when the pressure field is known or estimated can the momentum equations be solved.

Using the pressure field u^*, v^* and w^*, the resulting velocity field satisfies the continuity equation. Based on the guessed pressure field p*, The starred velocity field will result from the solution of the following discretization equations;

$$a_e u_e^* = \sum a_{nb} u_{nb}^* + b + (p_P^* - p_E^*) A_e \tag{4.20}$$

$$a_n v_n^* = \sum a_{nb} v_{nb}^* + b + (p_P^* - p_N^*) A_n \tag{4.21}$$

$$a_t w_t^* = \sum a_{nb} w_{nb}^* + b + (p_P^* - p_T^*) A_t \tag{4.22}$$

Where the location *t* lies on the *z* – direction grid line between grid points *P* and *T*.

4.6 The Pressure and Velocity Corrections

Our aim is to find a way of improving the guessed pressure p^* such that the resulting starred velocity field will progressively get closer to satisfying the continuity equation. Let the correct pressure p be obtained from;

$$p = p^* + p' \tag{4.23}$$

Where p' is the pressure correction. Next, we need to know how the velocity components respond to this change in pressure. The corresponding velocity corrections u^*, v^*, w^* can be introduced in a similar manner;

$$u = u^* + u', \qquad v = v^* + v', \qquad w = w^* + w' \tag{4.24}$$

When we subtract equations (4.20) from (4.17) we have;

$$a_e u_e - a_e u_e^* = \{\sum a_{nb} u_{nb} + b + (P_P - P_E)A_e\} - \{\sum a_{nb} u_{nb}^* + b + (p_p^* - p_E^*)A_e\} \quad (4.25)$$

Which results to;

$$a_e u_e' = \sum a_{nb} u_{nb}' + b + (p_p' - p_E')A_e \quad (4.26)$$

The PISO scheme we shall use approximates equation (4.26) by dropping of the term $\sum a_{nb} u_{nb}'$ from the equation for the following reasons;

i. PISO algorithm is an improvement on SAMPLE, which uses semi-implicit approach by dropping any term that would have an indirect influence of pressure correction on velocities
ii. On convergence, all the corrections tend to zero and there is no error induced on dropping $\sum a_{nb} u_{nb}'$ for obtaining the pressure equation.
iii. For computational convenience.
iv. Because PISO is an iterative method, there is no need for the formula used to forecast to be physically accurate.
v. To expedite the convergence of the velocity field to a solution that satisfies the continuity of equation, we are allowed to construct a formula for p' that is simply a numerical artifice.

The omission on equation (4.26) results to;

$$a_e u_e' = (p_p' - p_E')A_e \quad (4.27)$$

Dividing equation (4.27) through by a_e yields

$$u_e' = d_e(p_p' - p_E') \quad (4.28)$$

In which case

$$d_e \equiv \frac{A_e}{a_e} \tag{4.29}$$

Equation (4.28) will be called the velocity-correction formula. Using equation (4.24) we have;

$$u_e = u_e^* + u_e' \tag{4.30}$$

Replacing u_e' in equation (4.30), from equation (4.28) results to;

$$u_e = u_e^* + d_e\left(p_p' - p_E'\right) \tag{4.31}$$

This shows how the starred velocity u_e^* is to be corrected in response to the corrections to provide u_e. The correction formulae for the velocity components in other directions can be written similarly:

$$v_e = v_n^* + d_n\left(p_p' - p_N'\right) \tag{4.32}$$

$$w_t = w_t^* + d_t\left(p_p' - p_T'\right) \tag{4.33}$$

4.7 The Pressure Corrections Equation

We'll now convert the continuity equation into a pressure correction equation. For the purposes of this three-dimensional derivation, we will assume that density does not directly depend on pressure.

The continuity equation (3.1) can be written as;

$$\frac{\partial \rho}{\partial t} + \frac{\partial(\rho u)}{\partial x} + \frac{\partial(\rho v)}{\partial y} + \frac{\partial(\rho w)}{\partial z} = 0 \tag{4.34}$$

We shall integrate equation (4.34) over the shaded control volume in figure 4.2 with the following assumptions;

i. For the integration of the term $\frac{\partial \rho}{\partial t}$ we shall assume that the density ρ_P prevails over the control volume.

ii. Velocity components such as u_e located on a control volume surface will be supposed to govern the mass flow rate for the whole face.

With these assumptions, the integrated form of equation (4.34) becomes;

$$\frac{(\rho_P - \rho_P^0)\Delta x\Delta y\Delta z}{\Delta t} + [(\rho u)_e - (\rho u)_w]\Delta y\Delta z + [(\rho v)_n - (\rho v)_s]\Delta z\Delta x + [(\rho w)_t - (\rho w)_b]\Delta x\Delta y = 0 \quad (4.35)$$

Substituting for all the velocity components the expression given by the velocity-correction formulas, such as in equations (4.30)-(4.32) yields;

$$\frac{(\rho_P - \rho_P^0)\Delta x\Delta y\Delta z}{\Delta t} + \left[\rho_e\{u_e^* + d_e(p_p' - p_E')\} - \rho_w\{u_w^* + d_w(p_w' - p_P')\}\right]\Delta y\Delta z + \left[\rho_n\{v_n^* + d_n(p_p' - p_N')\} - \rho_n\{v_s^* + d_s(p_s' - p_P')\}\right]\Delta z\Delta x + \left[\rho_t\{w_t^* + d_t(p_p' - p_T')\} - \rho_b\{w_b^* + d_b(p_B' - p_P')\}\right]\Delta x\Delta y = 0 \quad (4.36)$$

Re-arranging equation (4.36) results to;

$$\frac{(\rho_P - \rho_P^0)\Delta x\Delta y\Delta z}{\Delta t} + [(\rho u^*)_e - (\rho u^*)_w]\Delta y\Delta z + [(\rho u^*)_n - (\rho u^*)_s]\Delta z\Delta x + [(\rho u^*)_t - (\rho u^*)_b] - \rho_e d_e p_E'\Delta y\Delta z - \rho_w d_w p_E'\Delta y\Delta z - \rho_n d_n p_N'\Delta z\Delta x - \rho_s d_s p_S'\Delta z\Delta x - \rho_t d_t p_T'\Delta x\Delta y - \rho_b d_b p_B'\Delta y\Delta z = -(\rho_e d_e\Delta y\Delta z + \rho_w d_w\Delta y\Delta z + \rho_n d_n p_N'\Delta z\Delta x + \rho_s d_s p_S'\Delta z\Delta x + \rho_t d_t p_T'\Delta x\Delta y + \rho_b d_b p_B'\Delta y\Delta z) \quad (4.37)$$

Multiplying equation (4.37) by negative one yields;

$$\frac{(\rho_P-\rho_P^0)\Delta x\Delta y\Delta z}{\Delta t}+[(\rho u^*)_w-(\rho u^*)_e]\Delta y\Delta z+[(\rho u^*)_s-(\rho u^*)_n]\Delta z\Delta x+[(\rho u^*)_b-(\rho u^*)_t]+$$

$$\rho_e d_e p'_E\Delta y\Delta z+\rho_w d_w p'_E\Delta y\Delta z+\rho_n d_n p'_N\Delta z\Delta x+\rho_s d_s p'_S\Delta z\Delta x+\rho_t d_t p'_T\Delta x\Delta y+$$

$$\rho_e d_e p'_E\Delta y\Delta z=-(\rho_e d_e\Delta y\Delta z+\rho_w d_w\Delta y\Delta z+\rho_n d_n\Delta z\Delta x+\rho_s d_s\Delta z\Delta x+\rho_t d_t\Delta x\Delta y+$$

$$\rho_b d_b\Delta x\Delta y)p'_p \qquad (4.38)$$

Re-arranging equation (4.38), we obtain the following discretization; equation for p';

$$a_P p'_P=a_E p'_E+a_W p'_W+a_N p'_N+a_S p'_S+a_T p'_T+a_B p'_B+b \qquad (4.39)$$

Where;

$$
\begin{aligned}
a_E &= \rho_e d_e \Delta y \Delta z \\
a_W &= \rho_w d_w \Delta y \Delta z \\
a_N &= \rho_n d_n \Delta z \Delta x \\
a_S &= \rho_s d_s \Delta z \Delta x \\
a_T &= \rho_t d_t \Delta x \Delta y \\
a_B &= \rho_b d_b \Delta x \Delta y \\
b &= \frac{(\rho_P - \rho_P^0)\Delta x \Delta y \Delta z}{\Delta t} + [(\rho u^*)_w - (\rho u^*)_e]\Delta y \Delta z + [(\rho v^*)_s - (\rho u^*)_n]\Delta z \Delta x \\
&\quad + [(\rho w^*)_b - (\rho w^*)_t]\Delta x \Delta y
\end{aligned}
\tag{4.40}
$$

Since the values of the density ρ will normally be available only at main grid points, the interface densities such as ρ_e may be calculated by any convenient interpolation. It can be seen from equation (4.40) that the left-hand side of the discretized continuity (4.35) evaluated in terms of getting the starred velocities is simply (the negative of) the term b in the pressure-correction equation As a result, we've written down all of the equations used to calculate the velocity components and pressure. In section 4, the PISO algorithm is used to solve equations (4.17), (4.18), and (4.19) discussed in (4.90).

4.8 The PISO Solution Algorithm

4.8.1 Predictor Step

The momentum equations can be solved only when the pressure field is given or is somehow estimated to initiate the PISO calculation process. The pressure field is estimated as p^* and the discretized momentum equations (4.17), (4.18) and (4.19) solved to yield an approximate velocity field component denoted by u^*, v^* and w^* as follows;

$$a_{i,j,k}u^*_{i,j,k} = \sum a_{nb}u^*_{nb} + \left(p^*_{i-1,j,k} - p^*_{i,j,k}\right)A_{i,j,k} + b_{i,j,k} \tag{4.41}$$

$$a_{i,j,k}v^*_{i,j,k} = \sum a_{nb}v^*_{nb} + \left(p^*_{i,j-1,k} - p^*_{i,j,k}\right)A_{i,j,k} + b_{i,j,k} \tag{4.42}$$

$$a_{i,j,k}w^*_{i,j,k} = \sum a_{nb}w^*_{nb} + \left(p^*_{i,j,k-1} - p^*_{i,j,k}\right)A_{i,j,k} + b_{i,j,k} \tag{4.43}$$

The initial guess for the pressure may be correct or not.

4.8.2 Corrector Step 1

Velocity component obtained from predictor step may not satisfy the continuity equation, so we define correction factor p', w', v' and u' for the pressure field and velocity field. Subtract the guessed pressure field p^* from the correct pressure field p^{**} to get the pressure correction factor p' as an equation (4.44);

$$p'_{i,j,k} = p^{**}_{i,j,k} - p^*_{i,j,k} \tag{4.44}$$

Using equation (4.28), (4.43) and applying the pressure correction factor to solve the momentum equation (4.17), the correction velocity components u^{**} , v^{**} and w^{**} are found as follows

$$u^{**}_{i,j,k} = u^*_{i,j,k} + d_{i,j,k}\left(p'_{i-1,j,k} - p'_{i,j,k}\right) \tag{4.45}$$

$$v_{i,j,k}^{**} = v_{i,j,k}^{*} + d_{i,j,k}\left(p'_{i,j-1,k} - p'_{i,j,k}\right) \tag{4.46}$$

$$w_{i,j,k}^{**} = w_{i,j,k}^{*} + d_{i,j,k}\left(p'_{i,j,k-1} - p'_{i,j,k}\right) \tag{4.47}$$

Where $p_{i,j,k}^{**}{}^{**}, u_{i,j,k}^{**}{}^{**}, v_{i,j,k}^{**}{}^{**}, w_{i,j,k}^{**}{}^{**}$: Correct pressure field and velocity components in the x, y and z directions respectively. The first discretized pressure equation is deduced from the momentum equations and the continuity equation and can be expressed as, Pantaker (1980);

$$a_P p_P = \sum a_{nb} p_{nb} + b_P \tag{4.48}$$

In this particular case the, basing on equation (4.48), the first correction equation into which mass fluxes as found at equations (4.45),(4.46), (4.47) are to be substituted to give the pressure correction factor, will be;

$$a_{i,j,k}p'_{i,j,k} = a_{i+1,j,k}p'_{i+1,j,k} + a_{i-1,j,k}p'_{i-1,j,k} + a_{i,j+1,k}p'_{i,j-1,k} + a_{i,j-1,k}p'_{i,j-1,k} + a_{i,j,k+1}p'_{i,j,k+1} + a_{i,j,k-1}p'_{i,j,k-1} + b'_{i,j,k} \tag{4.49}$$

With coefficient as given in equation (4.70)

4.8.3 Corrector Step 2

Using operator splitting technique, the second velocity correction field can be found as follows;

$$a_{i,j,k}u_{i,j,k}^{**} = \sum a_{nb}u_{nb}^{*} + \left(p_{i-1,j,k}^{**} - p_{i,j,k}^{**}\right)A_{i,j,k} + b_{i,j,k} \tag{4.50}$$

$$a_{i,j,k}v_{i,j,k}^{**} = \sum a_{nb}v_{nb}^{*} + \left(p_{i,j-1,k}^{**} - p_{i,j,k}^{**}\right)A_{i,j,k} + b_{i,j,k} \tag{4.51}$$

$$a_{i,j,k}w_{i,j,k}^{**} = \sum a_{nb}v_{nb}^{*} + \left(p_{i,j,k-1}^{*} - p_{i,j,k}^{**}\right)A_{i,j,k} + b_{i,j,k} \tag{4.52}$$

$$a_{i,j,k}u^{***}_{i,j,k} = \sum a_{nb}u^{**}_{nb} + \left(p^{***}_{i-1,j,k} - p^{***}_{i,j,k}\right)A_{i,j,k} + b_{i,j,k} \quad (4.53)$$

$$a_{i,j,k}v^{***}_{i,j,k} = \sum a_{nb}v^{**}_{nb} + \left(p^{***}_{i,j-1,k} - p^{***}_{i,j,k}\right)A_{i,j,k} + b_{i,j,k} \quad (4.54)$$

$$a_{i,j,k}w^{***}_{i,j,k} = \sum a_{nb}v^{**}_{nb} + \left(p^{***}_{i,j,k-1} - p^{***}_{i,j,k}\right)A_{i,j,k} + b_{i,j,k} \quad (4.55)$$

Note that the velocity in term on the right hand side and in the term on the left hand side are evaluated at different iteration levels, hence the algorithm is called "operator splitting PISO algorithm". Subtracting equations (4.50), (4.51) and (4.52) from equation (4.53), (4.54) and (4.55) respectively yields;

$$a_{i,j,k}u^{***}_{i,j,k} - a_{i,j,k}u^{**}_{i,j,k} = \sum(a_{nb}u^{**}_{nb} - a_{nb}u^{*}_{nb}) + \left(p^{***}_{i-1,j,k} - p^{***}_{i,j,k}\right)A_{i,j,k} - \left(p^{**}_{i-1,j,k} - p^{**}_{i,j,k}\right)A_{i,j,k} + b_{i,j,k} - b_{i,j,k} \quad (4.56)$$

$$a_{i,j,k}v^{***}_{i,j,k} - a_{i,j,k}v^{**}_{i,j,k} = \sum(a_{nb}v^{**}_{nb} - a_{nb}v^{*}_{nb}) + \left(p^{***}_{i,j-1,k} - p^{***}_{i,j,k}\right)A_{i,j,k} - \left(p^{**}_{i-1,j,k} - p^{**}_{i,j,k}\right)A_{i,j,k} + b_{i,j,k} - b_{i,j,k} \quad (4.57)$$

$$a_{i,j,k}w^{***}_{i,j,k} - a_{i,j,k}w^{**}_{i,j,k} = \sum(a_{nb}w^{**}_{nb} - a_{nb}w^{*}_{nb}) + \left(p^{***}_{i,j,k-1} - p^{***}_{i,j,k}\right)A_{i,j,k} - \left(p^{**}_{i,j,k-1} - p^{**}_{i,j,k}\right)A_{i,j,k} + b_{i,j,k} - b_{i,j,k} \quad (4.58)$$

Equation (4.56), (4.57) and (4.58) simplifies to;

$$a_{i,j,k}u^{***}_{i,j,k} = a_{i,j,k}u^{**}_{i,j,k} + \sum a_{nb}\left(u^{**}_{nb} - u^{*}_{nb}\right) + \left(p^{***}_{i-1,j,k} - p^{***}_{i,j,k}\right)A_{i,j,k} - \left(p^{**}_{i-1,j,k} - p^{**}_{i,j,k}\right)A_{i,j,k} + \left(p^{**}_{i-1,j,k} - p^{**}_{i,j,k}\right)A_{i,j,k} + b_{i,j,k} - b_{i,j,k} \quad (4.59)$$

$$a_{i,j,k}u^{***}_{i,j,k} = a_{i,j,k}v^{**}_{i,j,k} + \sum a_{nb}\left(v^{**}_{nb} - v^{*}_{nb}\right) + \left(p^{***}_{i,j-1,k} - p^{***}_{i,j,k}\right)A_{i,j,k} - \left(p^{**}_{i,j-1,k} - p^{**}_{i,j,k}\right)A_{i,j,k} + b_{i,j,k} - b_{i,j,k} \quad (4.60)$$

$$a_{i,j,k}w^{***}_{i,j,k} = a_{i,j,k}w^{**}_{i,j,k} + \sum a_{nb}\,(w^{**}_{nb} - w^{*}_{nb}) + \left(p^{***}_{i,j,k-1} - p^{***}_{i,j,k}\right)A_{i,j,k} - \left(p^{**}_{i,j,k-1} - p^{**}_{i,j,k}\right)A_{i,j,k} + b_{i,j,k} - b_{i,j,k} \quad (4.61)$$

Further simplification of equations (4.59), (4.60), and (4.61) results to;

$$u^{***}_{i,j,k} = u^{**}_{i,j,k} + \frac{\sum a_{nb}\left(u^{**}_{nb} - u^{*}_{nb}\right)}{a_{i,j,k}} + d_{i,j,k}\left(p''_{i-1,j,k} - p''_{i,j,k}\right) \quad (4.62)$$

$$v^{***}_{i,j,k} = v^{**}_{i,j,k} + \frac{\sum a_{nb}\left(v^{**}_{nb} - v^{*}_{nb}\right)}{a_{i,j,k}} + d_{i,j,k}\left(p''_{i,j-1,k} - p''_{i,j,k}\right) \quad (4.63)$$

$$w^{***}_{i,j,k} = w^{**}_{i,j,k} + \frac{\sum a_{nb}\left(w^{**}_{nb} - w^{*}_{nb}\right)}{a_{i,j,k}} + d_{i,j,k}\left(p''_{i,j,k-1} - p''_{i,j,k}\right) \quad (4.64)$$

Where $d_{i,j,k} = \frac{A_{i,j,k}}{a_{i,j,k}}$; $p^{***}, v^{***}, u^{***}$ are correct pressure field and velocity components respectively and p'', v'', u'' are second correction pressure and velocity field respectively.

Therefore using equations (4.44), (4.45), (4.46) and (4.47) pressure and velocities are corrected as follows;

$$p^{***}_{i,j,k} = p^{*}_{i,j,k} + p'_{i,j,k} + p''_{i,j,k} \quad (4.65)$$

$$u^{***}_{i,j,k} = u^{*}_{i,j,k} + d_{i,j,k}\left(p'_{i-1,j,k} - p'_{i,j,k}\right) + \frac{\sum a_{nb}\left(u^{**}_{nb} - u^{*}_{nb}\right)}{a_{i,j,k}} + d_{i,j,k}\left(p''_{i-1,j,k} - p''_{i,j,k}\right) \quad (4.66)$$

$$v^{**}_{i,j,k} = v^{*}_{i,j,k} + d_{i,j,k}\left(p'_{i,j-1,k} - p'_{i,j,k}\right) + \frac{\sum a_{nb}\left(v^{**}_{nb} - v^{*}_{nb}\right)}{a_{i,j,k}} + d_{i,j,k}\left(p''_{i,j-1,k} - p''_{i,j,k}\right) \quad (4.67)$$

$$w^{**}_{i,j,k} = w^{*}_{i,j,k} + d_{i,j,k}\left(p'_{i,j,k-1} - p'_{i,j,k}\right) + \frac{\sum a_{nb}\left(w^{**}_{nb} - w^{*}_{nb}\right)}{a_{i,j,k}} + d_{i,j,k}\left(p''_{i,j,k-1} - p''_{i,j,k}\right) \quad (4.68)$$

The discretized second pressure correction equation is deduced from the momentum equations and the continuity equation and can be expressed as, Panteker, (1980). In this particular case then, basing on equation (4.48), the second pressure correction equation into which mass fluxes as found at equation (4.66), (4.67), (4.68) are to be substituted to give the pressure correction factor, will be;

$$a_{i,j,k}p''_{i,j,k} = a_{i+1,j,k}p''_{i+1,j,k} + a_{i-1,j,k}p''_{i-1,j,k} + a_{i,j+1,k}p''_{i,j+1,k} + a_{i,j-1,k}p''_{i,j-1,k} + a_{i,j,k+1}p''_{i,j,k+1} + a_{i,j,k-1}p''_{i,j,k-1} + b''_{i,j,k} \quad (4.69)$$

Where;

$$a_{i+1,j,k} = (\rho dA)_{i+1,j,k}$$

$$a_{i-1,j,k} = (\rho dA)_{i-1,j,k}$$

$$a_{i,j+1,k} = (\rho dA)_{i,j+1,k}$$

$$a_{i,j-1,k} = (\rho dA)_{i,j-1,k}$$

$$a_{i,j,k+1} = (\rho dA)_{i,j,k+1}$$

$$a_{i,j,k-1} = (\rho dA)_{i,j,k-1}$$

$$a_{i+1,j,k} = a_{i+1,j,k} + a_{i-1,j,k} + a_{i,j+1,k} + a_{i,j-1,k} + a_{i,j,k+1} + a_{i,j,k-1}$$

$$b = (\frac{\rho A}{a})_{i,j,k} \sum a_{nb} (u_{nb}^{**} - u_{nb}^{*}) - (\frac{\rho A}{a})_{i+1,j,k} \sum a_{nb} (u_{nb}^{**} - u_{nb}^{*})$$
$$+ (\frac{\rho A}{a})_{i,j,k} \sum a_{nb} (v_{nb}^{**} - v_{nb}^{*}) - (\frac{\rho A}{a})_{i,j+1,k} \sum a_{nb} (v_{nb}^{**} - v_{nb}^{*})$$
$$+ (\frac{\rho A}{a})_{i,j,k} \sum a_{nb} (w_{nb}^{**} - w_{nb}^{*}) - (\frac{\rho A}{a})_{i,j,k+1} \sum a_{nb} (w_{nb}^{**} - w_{nb}^{*})$$

(4.70)

The solution algorithm can be summarized in a flow chart as illustrated in the next section.

4.9 PISO Flow Chart

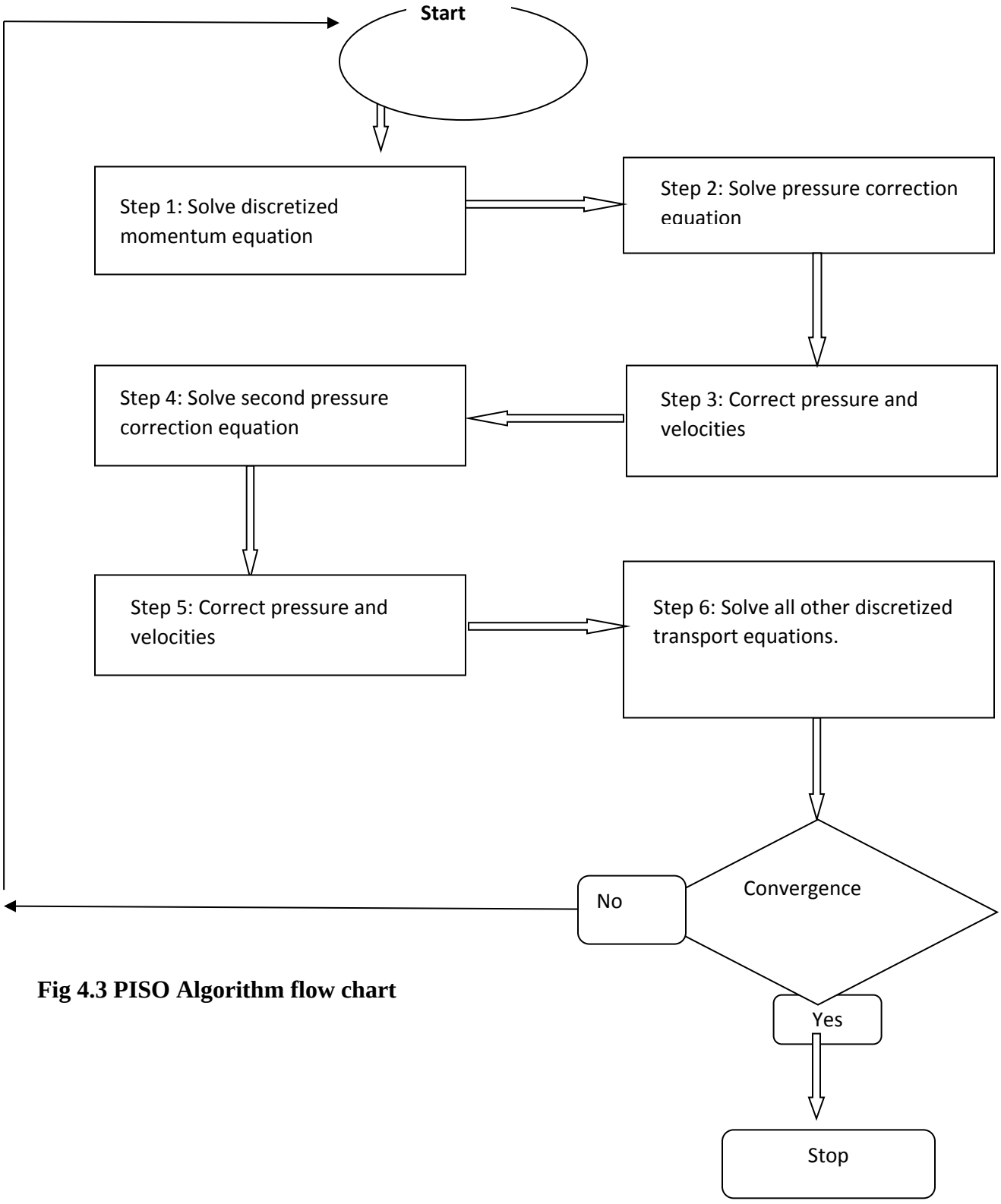

Fig 4.3 PISO Algorithm flow chart

CHAPTER FIVE

RESULTS AND DISCUSSION

The results presented here were obtained by solving equation (4.65), (4.66), (4.67) and (4.68) by PISO for turbulent natural convention of air in a 2-D enclosures of Rayleigh numbers between $10^9 to\ 10^{11}$ .The numerical results we have found with these boundary conditions are numerical solutions for variables in $\kappa - \omega$ model.

1.1 Grid Convergence

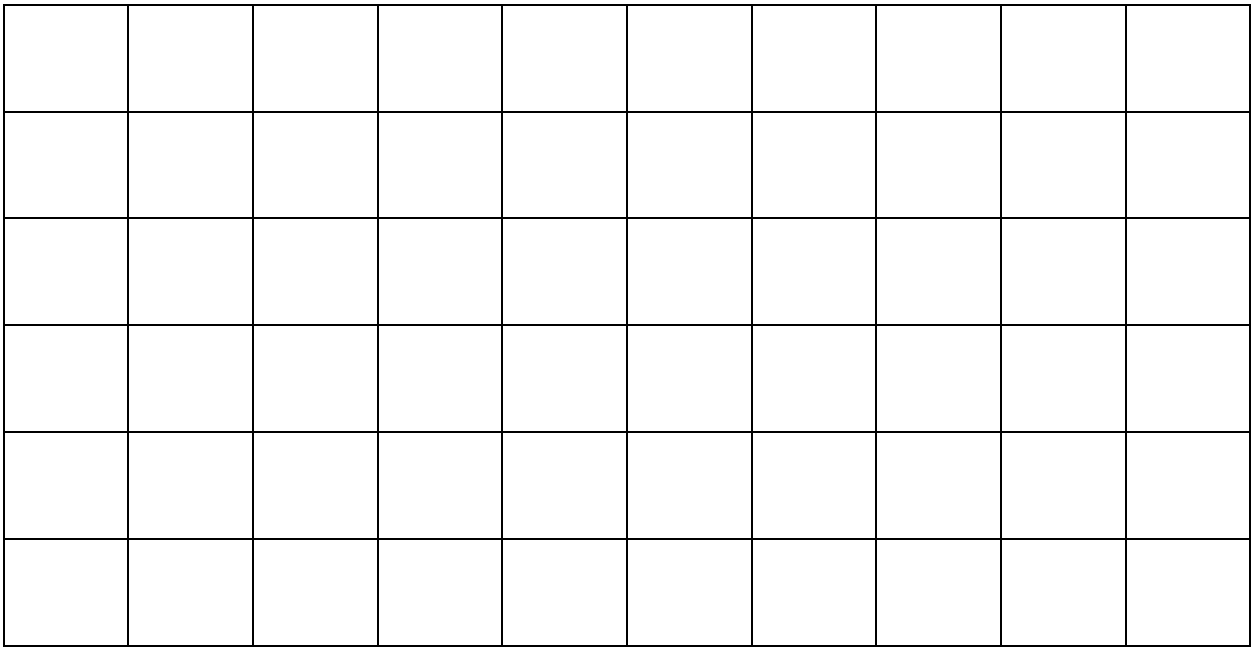

Fig 5.1 grid 40x40

In these validations, the grid shown in figure 5.1 is the standard grid. The staggered and grouped computing grids towered over the walls. Scalar variables such as pressure, temperature, density, and turbulent quantities are stored in the control volume's cell centers, while vector variables such as velocities and velocity are stored in the cell faces. This would result in a robust coupling between pressure and velocities. As a result of the odd-even decoupling, a discretization error that causes checker-board patterns in the solution, convergence occurs. The flow of turbulent natural

convention in an enclosure is characterized by a thin boundary layer along the walls, while the core is thermally stratified, so grids are grouped towards the wall. The flow gradients in the boundary layer are very large, necessitating a huge number of computing grids, the values of which must be determined in order to capture the flow physics.

5.1 Isotherms

Isotherm is a line of equal or constant temperature. It is a curve on a graph that connects points of equal temperature. In the fig.5.11 the maximum temperature is 285K, in fig 5.12 the maximum temperature is 254K and in fig 5.13 the maximum temperature is 227K.

There is high temperature on the left side of the wall. There is also rising up of hot less dense particles which loses its heat with distance as shown by change in colour. In between the two isotherm walls, there is mixing of air particles which is a relatively warm region achieving temperature uniformity. Therefore, maximum temperature decreases with increase in Rayleigh number as evident from the figures (fig 5.11, fig 5.12 and fig 5.13) shown below.

Fig 5.11 Isotherms of Rayleigh number 10^9

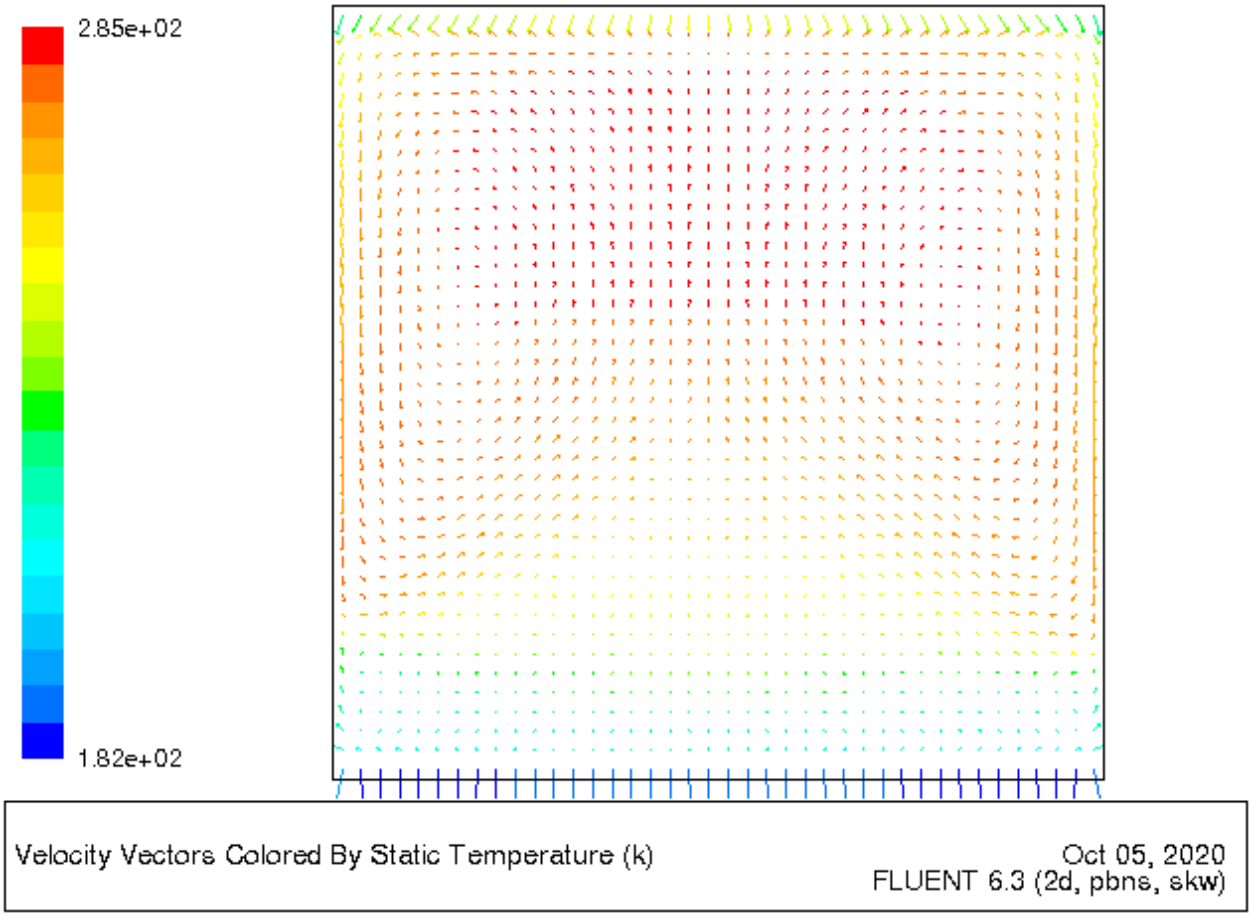

Fig 5.12 Isotherms of Rayleigh number 10^{10}

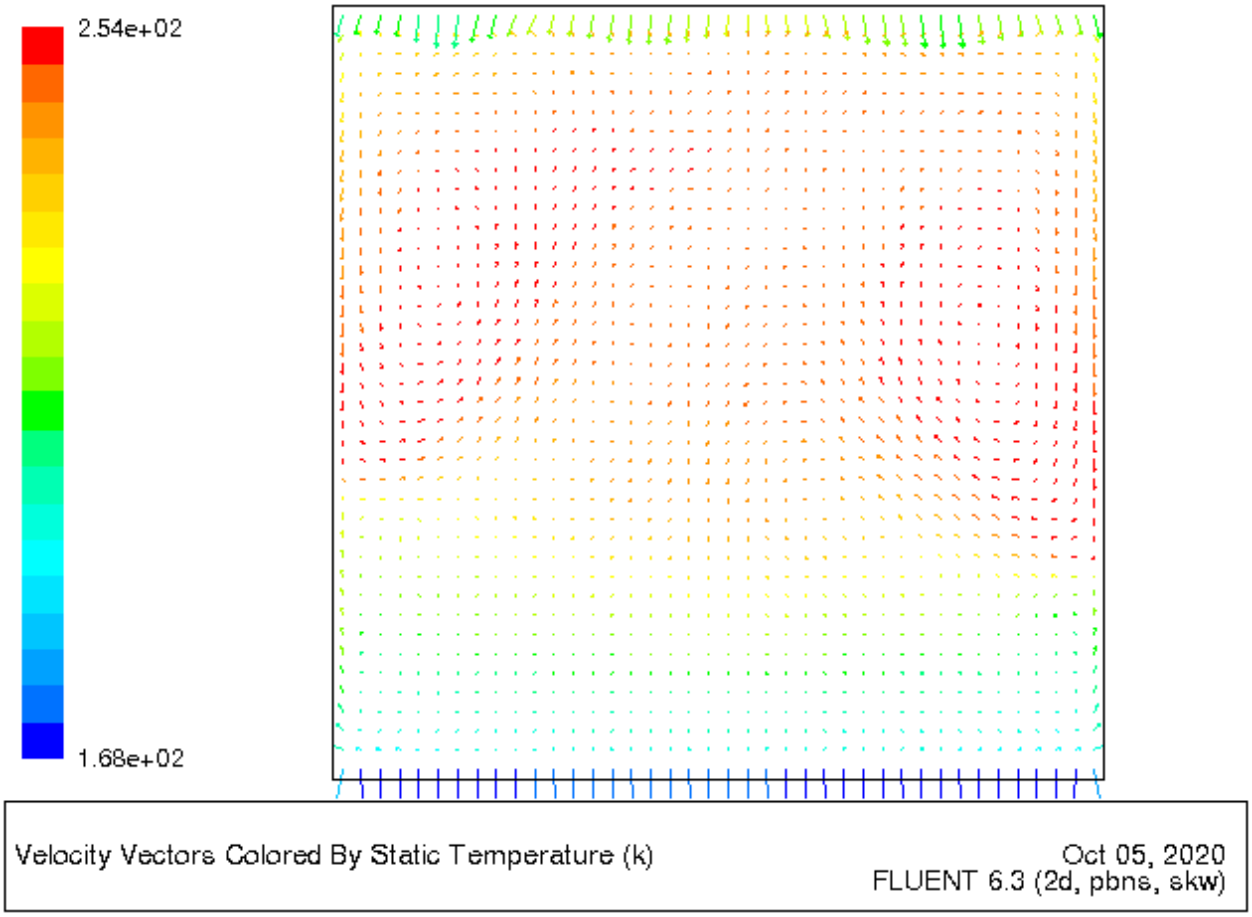

Fig 5.13 Isotherms of Rayleigh number 10^{11}

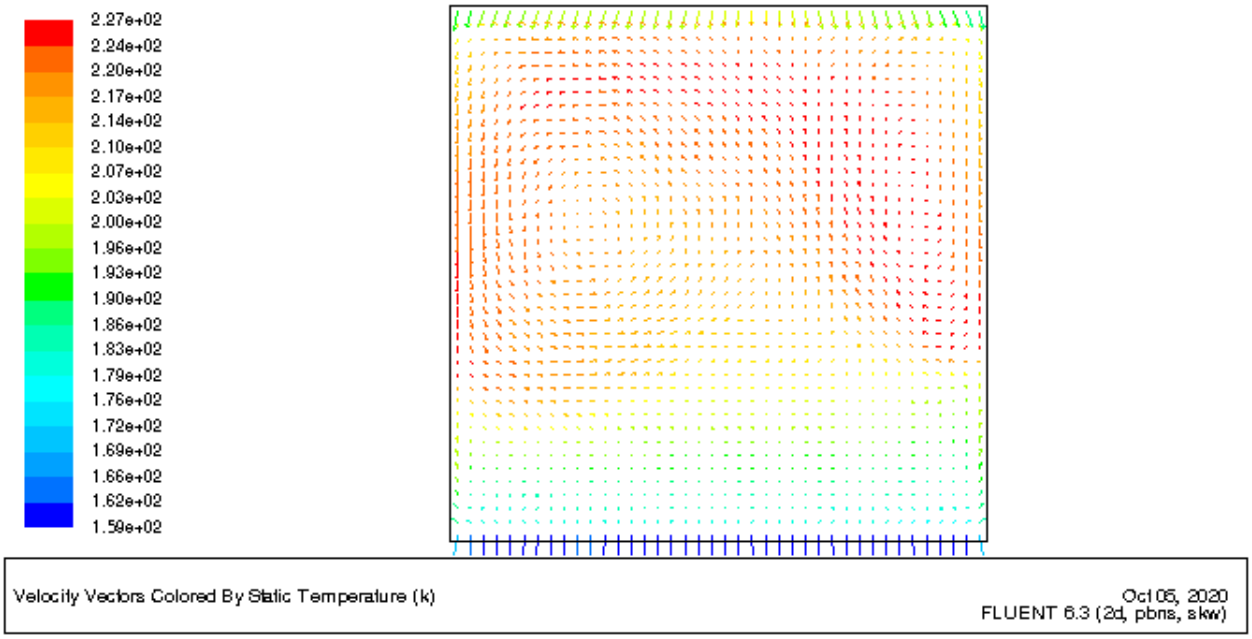

5.2 Contours of Velocity Magnitude

In fig 5.2.1, the highest velocity of air particles is 0.837m/s, in fig 5.2.2, the highest velocity is 1.25 m/s and in fig 5.2.3 the highest velocity is 1.87m/s, in fig 5.2.1 the highest speed is at the middle at the mixing region. Vortices are more in 5.2.1 which becomes parallel as the Rayleigh number increases in fig 5.2.3.The vortices are parallel than any other set-up in this study and at this point it is evident that as the Rayleigh number increases the flow becomes less turbulent.

Fig 5.2.1 Contours of velocity magnitude Rayleigh number 10^9

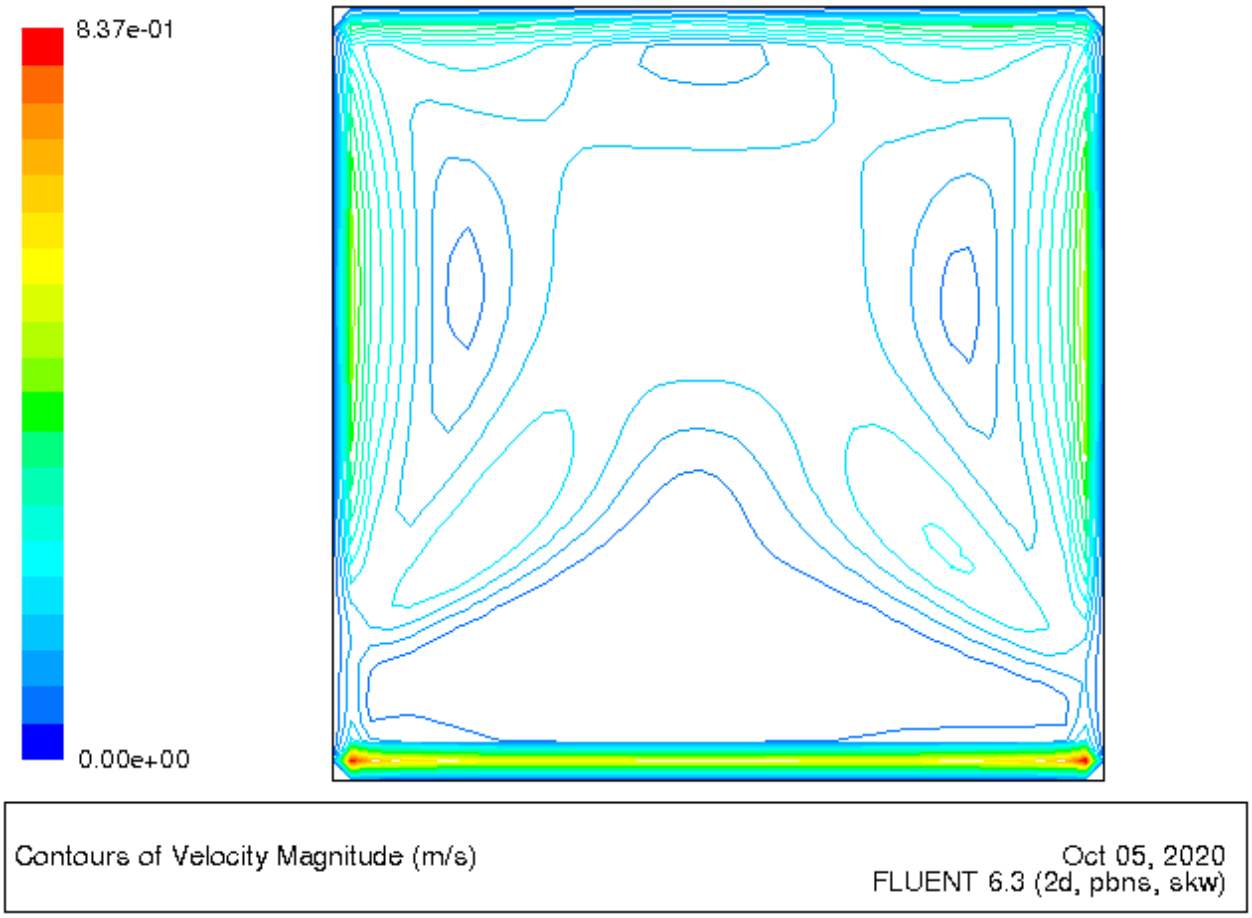

Fig 5.2.2 Contours of velocity magnitude Rayleigh number 10^{10}

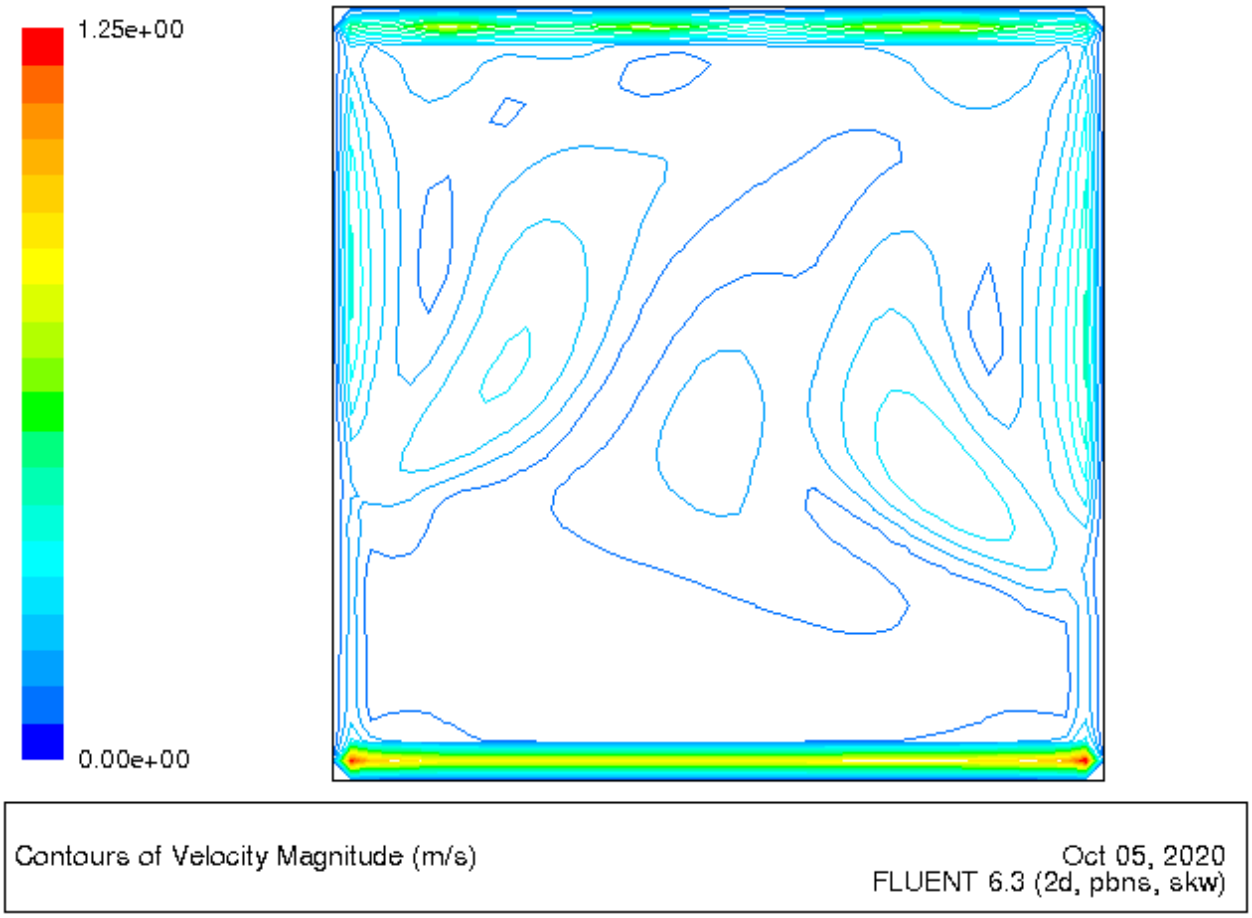

Fig 5.2.3 Contours of velocity magnitude Rayleigh number 10^{11}

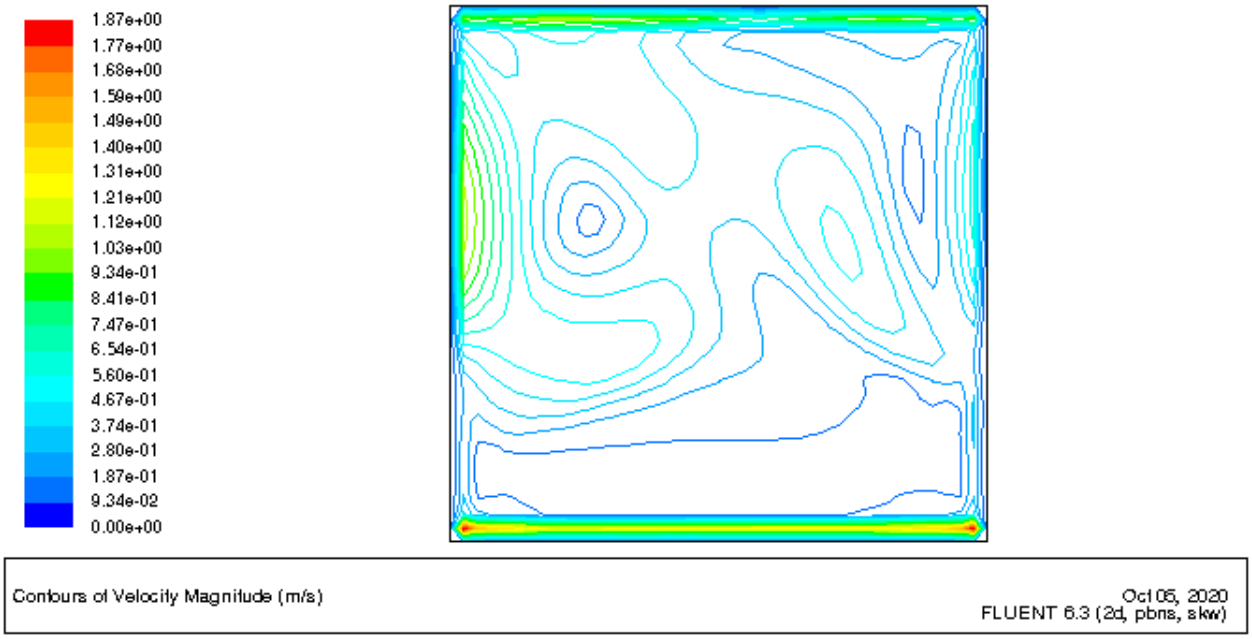

5.3 Streamline Distribution

Streamline is an imaginary line in a fluid such that the tangent at any point shows the path of the speed of an element of the fluid at that point. The lowest value indicated is of the Rayleigh number $\mathbf{10^9}$which is 0.09kg/s followed by that of Rayleigh number $\mathbf{10^{10}}$which is 0.154kg/s.This value increases as the Rayleigh number increases as depicted by that of a Rayleigh number $\mathbf{10^{11}}$ which is 0.852kg/s, In the fig.5.3.1, the vortices are big in size and they assume a circular part which deforms as distance increases from their centers. In fig 5.3.2, the radius of center circle reduces which as well decreases as the Rayleigh number increases to as seen in fig 5.3.3

Fig 5.3.1 Contours of streamline of Rayleigh 10^9

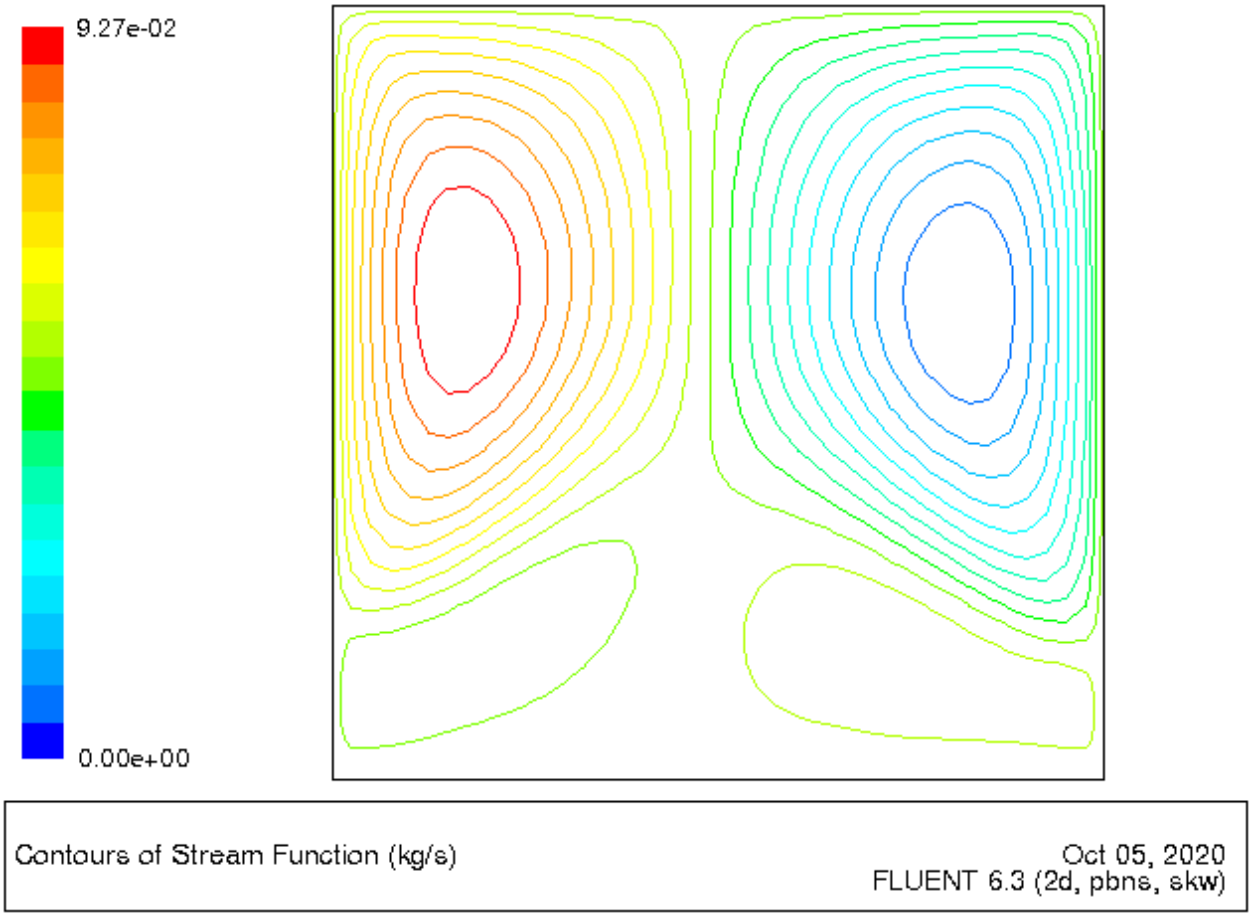

Fig 5.3.2 Contours of streamline of Rayleigh 10^{10}

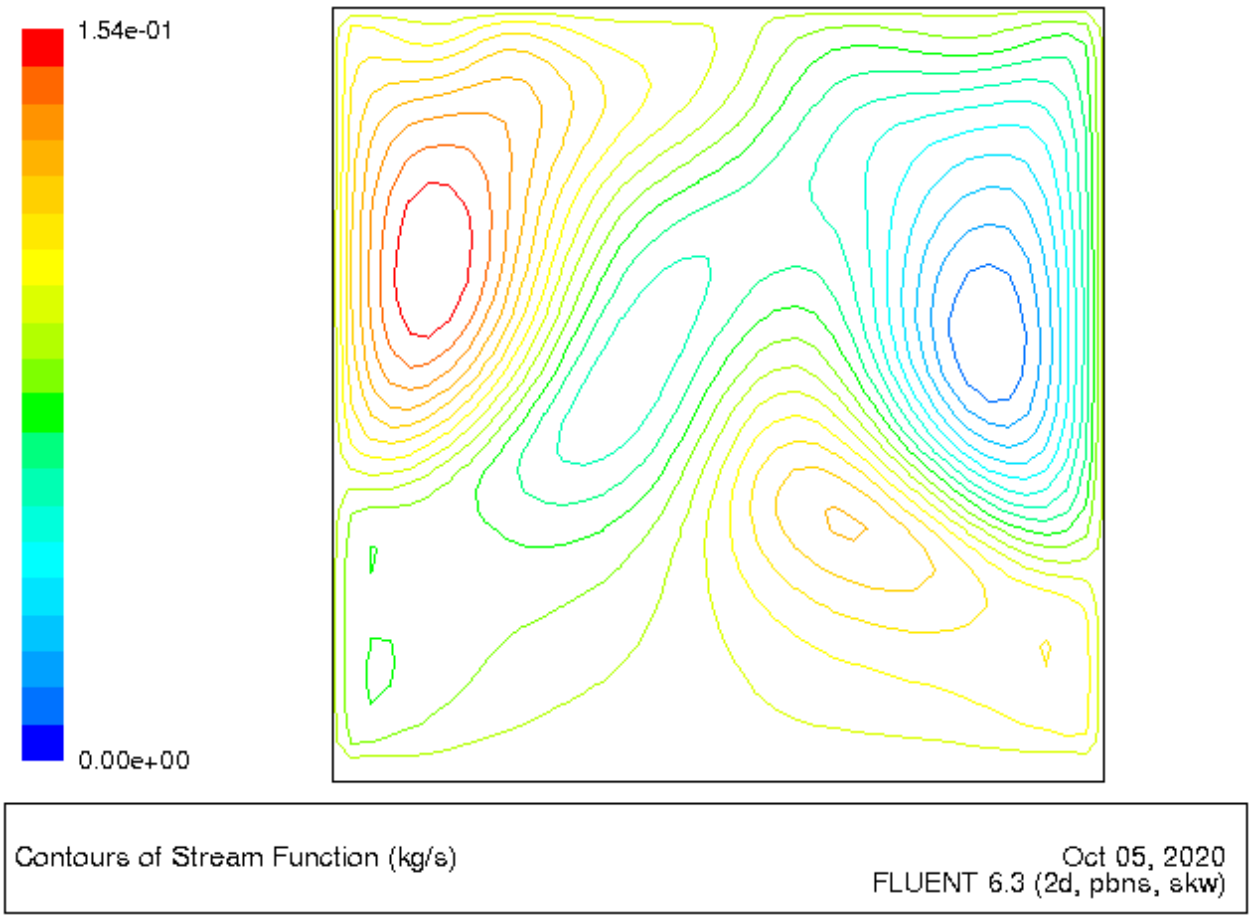

Fig 5.3.3 Contours of streamline of Rayleigh 10^{11}

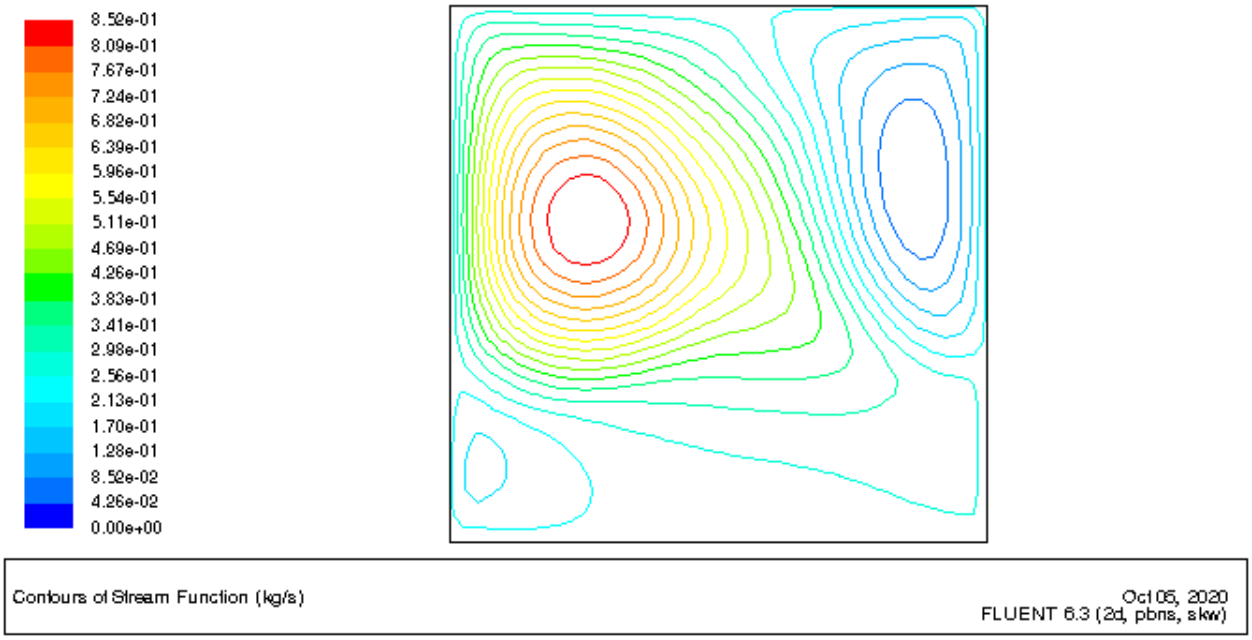

5.4 Conclusions

Based on the data from the simulations, the following conclusions were obtained;

a) Different temperature conditions resulted in two large cells in circular motions, both of which rotate in a clockwise direction.

b) Temperature profiles are important for thermal comfort (including air velocity, temperature and humidity levels), efficiency of energy balance and the effectiveness of the ventilation system when modeling air flow in buildings.

c) The flow is characterized by low Reynolds turbulence intensity and thermal stratification which provides thermal options of keeping items at the stated temperature in an enclosure without the use of an internal heat source.

d) The results obtained in the contours of velocity magnitude shows that as the Rayleigh number increases the flow becomes less turbulent.

5.5 Recommendations

Further investigations are recommended for;

1. Rectangular cavity using compressible fluids.
2. Enclosures with a two dimensional configurations

REFERENCES

Aithal S.M., (2016). Turbulent Natural Convection is a square cavity with a circular cylinder. Journal of Thermo physics and heat Transfer Vol 30 No 4, pp 843-853.

Awuor K. (2012), Turbulent Natural Convection in an Enclosure: Numerical Study of Different k-epsilon models, Ph.D. Thesis, Kenyatta University, Kenya, 1-102.

Boussinesq J. (1903), Th'eorie Analytique de la Chaleur, Gauthier-Villars, the *Astrophysical Journal*, **136,** 1126.

Cebeci T. and Smith A.M.O (1974), Analysis of Boundary Layers, Applied Mathematics and Mechanics, Academic Press, New York, **15,** 4-45.

Chai, X., Li, W., Chen, B., Liu, X., Xiong, J., & Cheng, X. (2020). Numerical simulation of turbulent natural convection in an enclosure with a curved surface heated from below. *Progress in Nuclear Energy*, *126*, 103392

Currie, I.G. (1974). Fundamental of Fluids, McGraw- Hill Inc.

Edward, M., Sigey, J., Okello, J., &Okwoyo, J. (2013).*Natural Convection with Localize Heating and Cooling on Opposite Vertical Walls in an Enclosure.CNCE, 1(4),* 72-78.

Gatheri F. K. (2005), Variable False Transient for the Solution of Coupled Elliptic Equations, *East African Journal of Physical Sciences,* **6** (2), 117.

Gatheri F. K., Reizes J., Leonardi E., and Graham V.D. (1994), Natural Convection in an Enclosure with Localized Heating and Cooling: A numerical Study, Heat Transfer, G.F. Hewitt, **2,** 361-366.

Goodarzi, M., Safaei, M. R., Karimipour, A., Hooman, K., Dahari, M., Kazi, S. N.,Sadeghinezhad, E. (2014).*Comparison of the finite volume and lattice Boltzmann methods for solving natural convection heat transfer problems inside cavities and enclosures*. In Abstract and Applied Analysis *(*Vol. 2014).Hindawi

Harlow F. H, Nakayama P. I. (1968), Transport of Turbulence Energy Decay Rate, Los Alamos Science Laboratory, LA-3854, 86-127.

Hatsopolous, G. N. and Keenan J. H. (1965), Principle of General Thermodynamic, John Wiley and Sons Inc., 123-190.

Jiyuan T., Guan H.Y. and Chaoqun L. (2012), Computational Fluid Dynamics, A Practical Approach, Elsevier Inc., **2,** 1-404.

Josephs K., Grace W.G., Francis K.G (2018). *A Numerical investigation of Turbulent Convection in 3-D Enclosure using $k-\omega SST$ model and SIMPLEC* Method.International Journal of Engineering Science and ResearchTechnology.

Kimunguyi, K.J. (2016). *A numerical investigation of turbulent natural convection in a 3-d enclosure using k-w SST model and PISO method* (Doctoral dissertation, Kenyatta University).

Pantaker S. V. (1980), Numerical Heat Transfer and Fluid Flow, Series in Computational Methods in Mechanics and Thermal Science, Hemisphere Publishing Corporation, **1**, 25-39.

Reynolds O. (1894), Dynamical theory of turbulent incompressible viscous fluids and the determination of the criterion Phil. Trans. R. Soc. London A, **186,** 123-161.

Sajjadi, H., &Kefayati, R. (2015*).* *Lattice Boltzmann simulation of turbulent natural convection in tall enclosure*s. Thermal Science*, 19(1),* 155-166.

Wilcox D. C. (1998), Turbulence modeling for computational Fluid Dynamics, DCW Industries Inc., Canada, 2, 103-217

Wu, T., & Lei, C. (2015).*On numerical modeling of conjugate turbulent natural convection and radiation in a differentially heated cavity.*International Journal of Heat andMass Transfer*, 91,* 454-446.

Zimmerman, C., &Groll, R. (2014).*Modeling turbulent heat transfer in a natural convection flow*.Journal of Applied Mathematics and Physics*, 2(07),* 662.